AD-A045 717 GENERAL SENSORS INC FORT WASHINGTON PA F/G 20/14
ANALYTICAL STUDY OF PASSIVE TECHNIQUES FOR MEASURING ATMOSPHERI--ETC(U)
OCT 77 H SADJIAN N62269-77-C-0058
UNCLASSIFIED GS-1-77-NADC NL

1 OF 1
ADA
045717

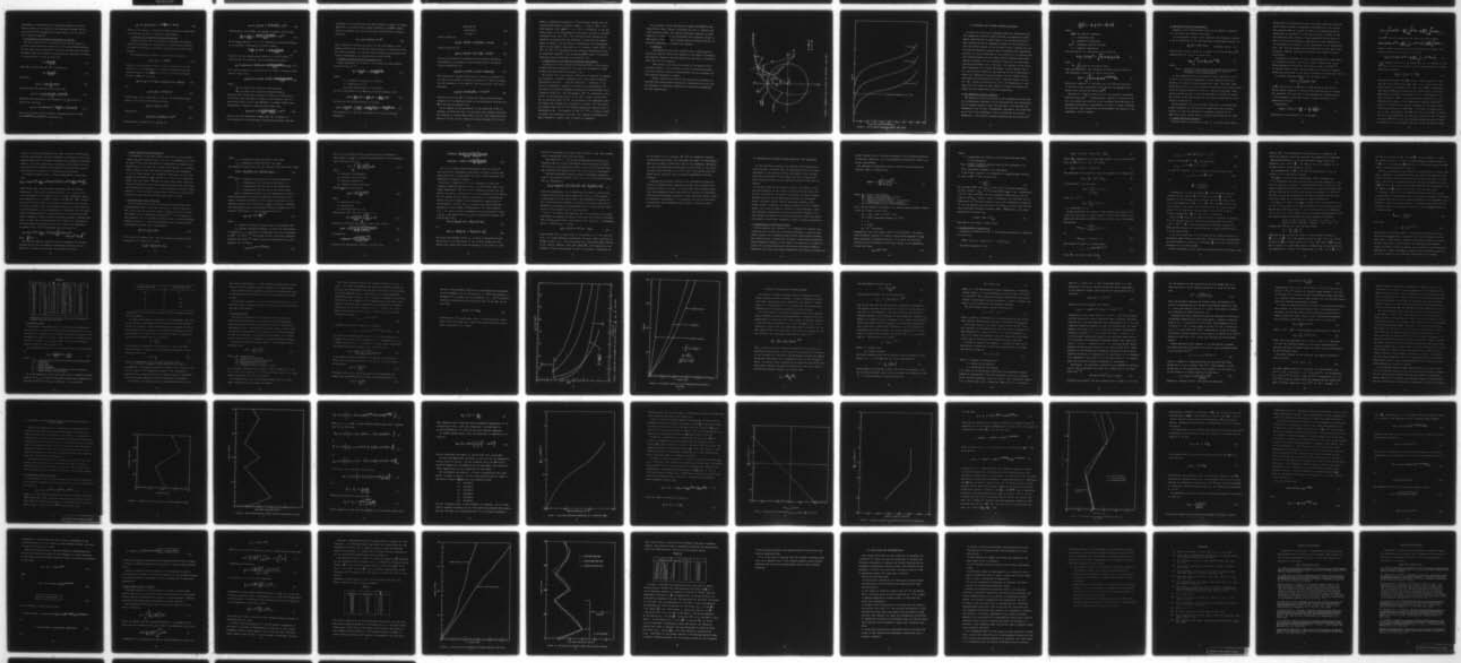

END
DATE FILMED
11-77
DDC

Report GS-NADC-1-77

GENERAL SENSORS, INC.

ANALYTICAL STUDY OF PASSIVE TECHNIQUES FOR MEASURING ATMOSPHERIC PARAMETERS

BY
Harry Sadjian
GENERAL SENSORS, INC.
500 Office Center Drive
Ft. Washington, Pa. 19034

6 October 1977

Final Report for Period 17 November 1976 - 6 September 1977

Approved for public release; distribution unlimited

Prepared for
NAVAL AIR DEVELOPMENT CENTER
Warminster, Pa. 18974

Copy No. 7

Report GS-NADC-1-77

ANALYTICAL STUDY OF PASSIVE TECHNIQUES FOR MEASURING ATMOSPHERIC PARAMETERS

BY
Harry Sadjian
GENERAL SENSORS, INC.
500 Office Center Drive
Ft. Washington, Pa. 19034

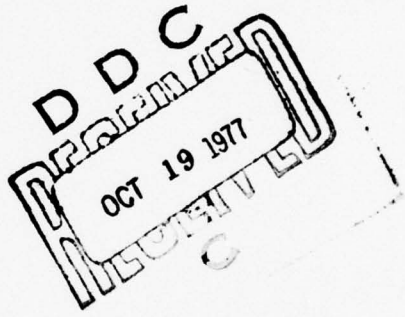

6 October 1977

Final Report for Period 17 November 1976 - 6 September 1977

Approved for public release; distribution unlimited

Prepared for
NAVAL AIR DEVELOPMENT CENTER
Warminster, Pa. 18974

See 1473

UNCLASSIFIED

SECURITY CLASSIFICATION OF THIS PAGE *(When Data Entered)*

REPORT DOCUMENTATION PAGE

READ INSTRUCTIONS BEFORE COMPLETING FORM

1. REPORT NUMBER: GS-~~NADC~~-1-77-NADC
2. GOVT ACCESSION NO.
3. RECIPIENT'S CATALOG NUMBER
4. TITLE *(and Subtitle)*: ANALYTICAL STUDY OF PASSIVE TECHNIQUES FOR MEASURING ATMOSPHERIC PARAMETERS,
5. TYPE OF REPORT & PERIOD COVERED: Final rept. 17 Nov ~~1976 to~~ 6 Sept 1977,
6. PERFORMING ORG. REPORT NUMBER
7. AUTHOR(s): Harry Sadjian
8. CONTRACT OR GRANT NUMBER(s): N62269-77-C-0058
9. PERFORMING ORGANIZATION NAME AND ADDRESS: General Sensors, Inc. 500 Office Center Drive Ft. Washington, Pa. 19034
10. PROGRAM ELEMENT, PROJECT, TASK AREA & WORK UNIT NUMBERS
11. CONTROLLING OFFICE NAME AND ADDRESS: Naval Air Development Center Warminster, Pa. 18974
12. REPORT DATE: 6 Oct 1977
13. NUMBER OF PAGES: ~~89~~ 88 p.
14. MONITORING AGENCY NAME & ADDRESS *(if different from Controlling Office)*
15. SECURITY CLASS. *(of this report)*: UNCLASSIFIED
15a. DECLASSIFICATION/DOWNGRADING SCHEDULE: N/A
16. DISTRIBUTION STATEMENT *(of this Report)*
17. DISTRIBUTION STATEMENT *(of the abstract entered in Block 20, if different from Report)*
18. SUPPLEMENTARY NOTES
19. KEY WORDS *(Continue on reverse side if necessary and identify by block number)*
Water-vapor distribution
Temperature distribution
Atmospheric infrared radiometry
Atmospheric microwave radiometry
Effect of water-vapor on radio wave propagation
20. ABSTRACT *(Continue on reverse side if necessary and identify by block number)*

Calculations are presented that show the degree of recovery of both atmospheric water-vapor and temperature distributions using passive infrared and microwave radiometry-assuming ground-based radiometers. A gradient technique is used to recover a temperature profile with 2 inversions and a water-vapor profile with 5 inversions. The method is applicable to distributions to 2 Km. Calculations are also presented that show the affect of water-vapor over →

DD FORM 1 JAN 73 1473 EDITION OF 1 NOV 65 IS OBSOLETE

UNCLASSIFIED 410 437

SECURITY CLASSIFICATION OF THIS PAGE *(When Data Entered)*

20. ABSTRACT (Continued)

and temperature on radio wave propagation and the affect of visibility on the passive methods.

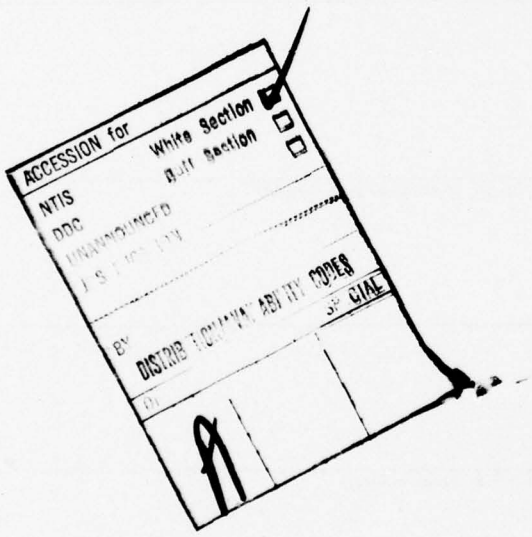

GS-NADC-1-77 6 October 1977

ANALYTICAL STUDY OF PASSIVE TECHNIQUES FOR MEASURING ATMOSPHERIC PARAMETERS

The reliability of received radar signals at sea is dependent on the reliable mapping of the atmospheric radio refractive index. The major component of the atmosphere that produces the unpredictable variation in the radio refractive index is due to the water-vapor distribution. This study was performed to determine the ability of passive infrared and microwave radiometry (using ground-based radiometers) to recover both the vertical distributions of water-vapor and temperature. Calculations are presented that indicate that the expected recovery is sufficiently accurate to predict the radio wave trajectory in a marine environment. As a worse case, the expected recovery for a water-vapor distribution containing 5 inversions and a temperature distribution containing 2 inversions is presented. This technique utilizes a gradient method and is applicable for distributions to 2 Km. Based on the calculated recoveries, recommendations are made to design a system interfaced with a microcomputer/controller that will be able to measure both the water-vapor and temperature distributions in real-time. This work was performed for the Naval Air Development Center in Warminster, Pa. under contract No. N62269-77-C-0058.

Grateful acknowledgement is given to Professor Gui A. Saatdjian of Drexel University for programming the equations and for his many and useful discussions concerning approach used during the course of this work. In addition, we are pleased to acknowledge the encouragement and guidance provided by Mr. Kenneth Petri of the Naval Air Development Center, the project monitor of this study.

CONTENTS

I INTRODUCTION

The accuracy and reliability of data from microwave radars can be improved if amplitude and angle corrections are applied to the received radar signals. Such corrections can be computed if the radio refractive index profile along the various propagation paths is available.

Naval studies have shown that the most difficult problem in reliable mapping of the atmospheric radio refractive index is the forecasting of the water-vapor distribution along the line of sight between the target and the transmitter. Accurate forecasting of the water-vapor concentration is difficult because of inadequate knowledge of the water-vapor's distribution at any given time and because of the difficulty in predicting vertical atmospheric motions which, to a large extent, control the changes in the water-vapor distribution. The verical motions that cause major changes in the water-vapor distribution are usually small, cannot generally be measured and must be inferred from large scale horizontal flow fields.

The simultaneous measurement of temperature has been identified as a significant secondary parameter of interest to the Navy. Present techniques for the measurement of water-vapor and temperature in the atmosphere utilize radiosondes (ballon launched and air dropped). In addition to requiring the use of expendables, radiosonde techniques are deficient because they are volume and direction limited. The volume of atmospheric coverage of radiosondes is not sufficient to perform adequate mapping of spatial

and temporal features important to radio meteorology. The radiosonde vertical profiles are too few and far between and do not sample in real time the volume of the atmosphere for which refractive index corrections are required.

Although currently, the Navy is investigating the use of Lidar as a viable means of determining the vertical water-vapor distribution in the atmosphere, this study is addressed to the ability of passive infrared and microwave radiometry to extract the same information.

The relative merits of active and passive methods are not the subject of this study; however, it is believed that ultimately the passive system will be found to be less expensive and bulky than the Lidar system while providing adequate mapping of the water-vapor distribution necessary for radar propagation corrections.

In order to assess the adequacy of the passive method, section II analyzes the degree of spatial resolution required to adequately describe radio wave propagation.

II SPATIAL RESOLUTION REQUIREMENTS FOR DESCRIBING RADIO WAVE PROPAGATION

This section establishes the guidelines for determining the spatial resolution requirements necessary to adequately describe radio wave propagation through the atmosphere whose water-vapor and temperature distributions are changing in time and space. These guidelines are necessary to properly assess whether a passive system can adequately recover the water-vapor and temperature profiles. The degree of recovery required will be dictated by the degree of recovery necessary to adequately describe the radio wave trajectory.

Due to the variety and magnitude of meteorological variables involved, we have made the following assumptions which are considered realistic:

(a) All refractive index gradients are normal to the earth's surface and are a function of the radial distance only

(b) The verical gradients do not change with horizontal extent (for distances to 10 Km; this is considered reasonable for a marine environment)

(c) Radio wavelengths of 6mm or greater are being utilized

(d) The radio wave refractive index is affected by temperature, water-vapor and pressure only (i.e. cloudless)

(e) The radio wave propagation can be described accurately by geometric optics

With these assumptions in mind, we proceed to derive the radius of curvature of a radio wave ray.

A. Derivation Of The Radius Of Curvature

The vector differential form of the path of rays in an inhomogeneous medium is given by,[1]

$$\frac{d}{ds}\left(n\frac{d\vec{r}}{ds}\right) = \nabla n \tag{1}$$

where s= distance along ray

n= refractive index, a function of r

r= radius vector

∇n= gradient of n

Expanding we have that,

$$\frac{dn}{ds}\cdot\frac{d\vec{r}}{ds} + n\frac{d^2\vec{r}}{ds^2} = \nabla n \tag{2}$$

We identify $d\vec{r}/ds = \hat{t}$ (unit vector tangent to the s direction, see Figure 1).

Consequently,

$$\hat{t}\frac{dn}{ds} + n\frac{d^2\vec{r}}{ds^2} = \nabla n \tag{3}$$

For a spherically symmetrical medium in which $\nabla n = \hat{r}\, dn/dr$ ($\hat{r}$ the unit vector in the r direction), assumption (a) above, we have that,

$$\hat{t}\frac{dn}{ds} + n\frac{d^2\vec{r}}{ds^2} = \hat{r}\frac{dn}{dr} \tag{4}$$

We identify the term $d\vec{r}/ds^2$ with $\vec{K}$, the curvature vector, whose magnitude is $1/\rho$, ρ the radius of curvature and whose direction is perpendicular to $\hat{t}$.

After rearranging, equation (4) becomes,

$$n\vec{K} = \hat{r}\frac{dn}{dr} - \frac{dn}{ds}\hat{t} \tag{5}$$

Multiplying through by $\vec{K}$ we have,

$$n|K|^2 = \frac{dn}{dr}\hat{r}\cdot\vec{K} - \hat{t}\cdot\vec{K}\frac{dn}{ds} \tag{6}$$

As $\vec{K}$ is perpendicular to $\hat{t}$, this becomes,

$$n|K|^2 = \frac{dn}{dr}\hat{r}\cdot\vec{K} \tag{7}$$

or

$$n\frac{1}{\rho^2} = \frac{dn}{dr}\cdot\frac{1}{\rho}\cos\beta \tag{8}$$

with β = the angle between $\hat{r}$ and $\vec{K}$. Since n is close to one, we have that,

$$\frac{1}{\rho} \approx \frac{dn}{dr}\cos\beta \tag{9}$$

From Figure 1, $\alpha = \beta$, where α is the angle the ray makes with the local horizon. Finally we have that,

$$\frac{1}{\rho} \approx \frac{dn}{dr}\cos\alpha \tag{10}$$

For a spherically symmetric distribution, the ray is a part of a circle whose radius is ρ and is confined to a plane formed by the initial ray direction. The derivation of the coordinates of the center of the ρ-circle is found to be,

$$a = \rho\sin\alpha \tag{11}$$

$$b = R - \rho\cos\alpha \tag{12}$$

Consequently, given α and dn/dr (constant gradient) with the earth's center at the center of the coordinate system, the ray trajectory follows the ρ-circle whose center is at +a and -b for a negative gradient.

B. Derivation of the Angular Variation of the Ray

The fact that the ray is confined to move along the arc of a great circle allows the derivation of the relationship between Υ, the angle the ray makes with the local horizon, and the known variables using only geometric considerations. Referring to Figure 1, using the law of sines we have that,

$$X = \frac{R \sin \theta}{\sin \delta} \tag{13}$$

where $\delta = 180 - \epsilon$ with $\epsilon = \alpha + \theta$. Consequently,

$$X = \frac{R \sin \theta}{\sin \epsilon} \tag{14}$$

Similarly,

$$\sin \Upsilon = \frac{(\rho - X) \sin \epsilon}{\rho} \tag{15}$$

Substituting from equation (14) we have that,

$$\sin \Upsilon = \frac{\rho \sin(\alpha + \theta) - R \sin \theta}{\rho} \tag{16}$$

Expanding and substituting the expression for ρ derived in section IA, we obtain,

$$\sin \Upsilon = \sin \theta \cos \alpha \left(1 - R \frac{dn}{dr}\right) + \sin \alpha \cos \theta \tag{17}$$

As we are concerned with horizontal distances only up to 10KM, then $\sin \theta \cong \theta$ and $\cos \theta \cong 1$ resulting in,

$$\sin \gamma = \theta \cos \alpha \left(1 - R \frac{dn}{dr}\right) + \sin \alpha \qquad (18)$$

Equation (18) implies a negative gradient and will be used below to calculate the spatial resolution requirements.

C. Derivation of Spatial Resolution Equations

Before equation (18) can be used to determine the spatial resolution requirements, expressions for dn/dr must be derived in terms of variations in pressure, temperature and water vapor pressure.

The instantaneous refractive index can be written as,

$$n = n_o + \delta(n_o) \qquad (19)$$

where n_o = the refractive index of some reference set of conditions (e.g. no atmosphere or a standard atmosphere with 60% relative humidity) and $\delta(n_o)$ = the variation from the reference. Letting $dn \cong \Delta n$ we have that,

$$\Delta n = n_2 - n_1 = n_{2,o} + \delta(n_{2,o}) - n_{1,o} - \delta(n_{1,o}) \qquad (20)$$

or,

$$\Delta n = \Delta n_o + \delta(\Delta n_o) \qquad (21)$$

However, Δn_o can be expressed in terms of the refractive index modulus N as used by meteorologists where,

$$\Delta n_o = \Delta N_o \times 10^{-6} \qquad (22)$$

Consequently,

$$\delta(\Delta n_o) = \delta(\Delta N_o) \times 10^{-6} \qquad (23)$$

Substituting in equation (21) results in,

$$\Delta n = \left\{ \Delta N_o + \delta(\Delta N_o) \right\} \times 10^{-6} \qquad (24)$$

Additionally, as $dr \cong \Delta H$, the change in height, we have that,

$$\frac{dn}{dr} \approx \frac{\Delta n}{\Delta H} = \frac{\left\{ \Delta N_o + \delta(\Delta N_o) \right\}}{\Delta H} \times 10^{-6} \qquad (25)$$

We call $\Delta N_o / \Delta H \times 10^{-6}$, K , as it represents a constant gradient or no gradient. Consequently, R dn/dr becomes,

$$R \frac{dn}{dr} \approx RK + \frac{6.371\, \delta(\Delta N_o)}{\Delta H} \qquad (26)$$

where we use the average earth radius as 6.371×10^6 meters [2].

Substituting into equation (18) and expanding we obtain,

$$\sin \Upsilon = \theta \cos \alpha - \theta RK \cos \alpha - \frac{6.371\, \theta \cos \alpha\, \delta(\Delta N_o)}{\Delta H} + \sin \alpha \qquad (27)$$

As we are interested in the deviation of Υ from a reference gradient we obtain that,

$$\Delta(\sin \Upsilon) = \sin \Upsilon_o - \sin \Upsilon_\delta = \frac{6.371\, \theta \cos \alpha\, \delta(\Delta N_o)}{\Delta H} \qquad (28)$$

where,

Υ_o = ray angle with reference fixed gradient

Υ_δ = ray angle with fixed and variable gradient

Equation (28) relates the deviation in Υ due to a deviation in N from the fixed reference. In order to put equation (28) in a more useful form, we note that $\theta \cos \alpha = H \cos \alpha / R \tan \alpha$ of the disturbance of extent H. Substituting we have that,

$$\Delta(\sin \Upsilon) = \frac{H\, \delta(\Delta N_o) \cos \alpha}{\Delta H \quad + \tan \alpha} \times 10^{-6} \qquad (29)$$

We will call the expression $H\, \delta(\Delta N_o) / \Delta H$, τ, a measure of the intensity of the disturbance causing the deviation from the

reference. As we are dealing with small changes in angle, we equate $\Delta(\sin\gamma)$ to $d(\sin\gamma)$ which equals $\cos\gamma d\gamma$ or $\cos\gamma\Delta\gamma$. Substituting in equation (29) and noting that $\cos\alpha \cong \cos\gamma$ we finally have that,

$$\tau = \Delta\gamma \tan\alpha \times 10^6 \tag{30}$$

This relates the strength and extent of the disturbance to the change in γ that can be tolerated and the angle of elevation of the ray. Before equation (30) can be used to determine the spatial resolution requirements, an estimate must be made of τ.

D. Effect of Meteorological Variables on N

Under assumption (c) of part A, the refractive index modulus can be written as [3],

$$N = \frac{77.6\,P}{T} + \frac{373{,}256\,P_w}{T^2} \tag{31}$$

where,

P = atmospheric pressure in millibars

T = temperature in ^{o}K

P_w = water vapor pressure in millibars

As we are interested in the ΔN due to these variables then,

$$\Delta N \approx \frac{\partial N}{\partial P}\Delta P + \frac{\partial N}{\partial T}\Delta T + \frac{\partial N}{\partial P_w}\Delta P_w \tag{32}$$

Carrying out the differentiation, we obtain,

$$\Delta N = \frac{77.6\,\Delta P}{T} - \left\{\frac{77.6\,P}{T^2} + \frac{746{,}512\,P_w}{T^3}\right\}\Delta T + \frac{373{,}256}{T^2}\Delta P_w \tag{33}$$

For heights up to 2 KM, the variation in P,T, and P_w are approximately,

$$1020 < P > 750$$
$$315 < T > 270 \qquad (34)$$
$$30 < P_w > 3$$

For hot humid air,

$$\Delta N = .25\,\Delta P + 3.76\,\Delta P_w - 1.51\,\Delta T \qquad (35)$$

and for cool dry air,

$$\Delta N = .29\,\Delta P + 5.71\,\Delta P_w - .91\,\Delta T \qquad (36)$$

As we are interested in estimates of the spatial resolution requirements, we average the two extremes and let the deviation be represented by,

$$\langle \Delta N \rangle = .27\,\Delta P - 1.21\,\Delta T + 4.44\,\Delta P_w \qquad (37)$$

This infers that the ΔN change with P,T and P_w is constant up to 2 KM. As the effect of pressure relative to T and P_w is small, for the estimation of the spatial resolution we will use the expression,

$$\langle \Delta N \rangle = 4.44\,\Delta P_w - 1.21\,\Delta T \qquad (38)$$

Dividing this by the ΔH in which this change occurs and multiplying by H the physical extent of the disturbance provides the τ to be used in equation (30).

As an example of the calculation of the magnitude of τ, we consider an inversion layer. An inversion layer usually indicates the presence of a humid mass under a dry one. The transition from humid air to dry air air causes the largest change in N. For ex-

ample, a temperature inversion of 2°/100 meters located near the ground would produce a change of $\Delta P_w = -.3$ and a $\Delta T = .02$. From equation (38), $\langle \Delta N \rangle = -1.33 - .02 = -1.35$/meter. If the physical extent of the disturbance is 200 meters (typical of the Mediterranean area) then $\tau = -270$. The minus sign indicating the direction of change from the reference. If more than one disturbance is present, the the effect is additive as the displacement effect is negligible. Consequently, we consider a range of $\tau = 1$ to $\tau = 10^4$. $\tau = 10^4$ representing very unusuall conditions and must be considered atypical. If an acceptable $\Delta\gamma$ is known, the spatial resolution can be determined from equation (30).

E. Calculation of the Spatial Resolution Requirements

In Figure 2, we have plotted log τ against α for three angles of $\Delta\gamma$ considered appropriate for radio wave propagation. These curves were calculated from equation (30).

We consider first what spatial resolution is required to adequately determine a standard atmosphere with a 60% relative humidity. Calculation indicates that the $\Delta N / \Delta H = -.04$/meter. If we use as a reference no gradient (straight line trajectories), we can treat the standard atmosphere gradient as the disturbance with a physical extent of 2 KM. Consequently, $\tau = 80$. Referring to Figure 2, if the tracking error is to be $.01^{\circ}$ or less, we find that for an elevation angle of 25°, the presence of the atmosphere does not effect the straight line trajectory to within $.01^{\circ}$. For elevation angles less than 25°, the spatial resolution required will be determined by α . For example, at $\alpha = 1^{\circ}$, $\tau = 3$. Hence in order to predict the trajectory to within $.01^{\circ}$, spatial measurements of about 2000/80/3 or about every 74 meters is necessary.

For inversion layers and humid air masses where τ could approach 1000 or more, Figure 2 indicates that for a .01° error and a 45° elevation angle, the spatial resolution required is 1000/1000/175= 175 meters if the disturbance has a physical extent of 1000 meters. Other elevation angles require different spatial resolution measurements to define the gradient.

F. Analysis

The examples cited above indicate that a single spatial resolution does not suffice but depends on the angle of elevation, the gradient caused by the disturbance and the error in refracted angle that can be tolerated.

Additionally, for elevation angles 30° or greater with a tolerable angle of .1° or greater; no set of inversion requires any better spatial resolution measurements than are necessary for the standard atmospheric gradient.

Unless trajectories close to the horizon are required, we conclude that coarse spatial resolution measurements are all that are necassary to adequately describe the radio wave propagation for most applications.

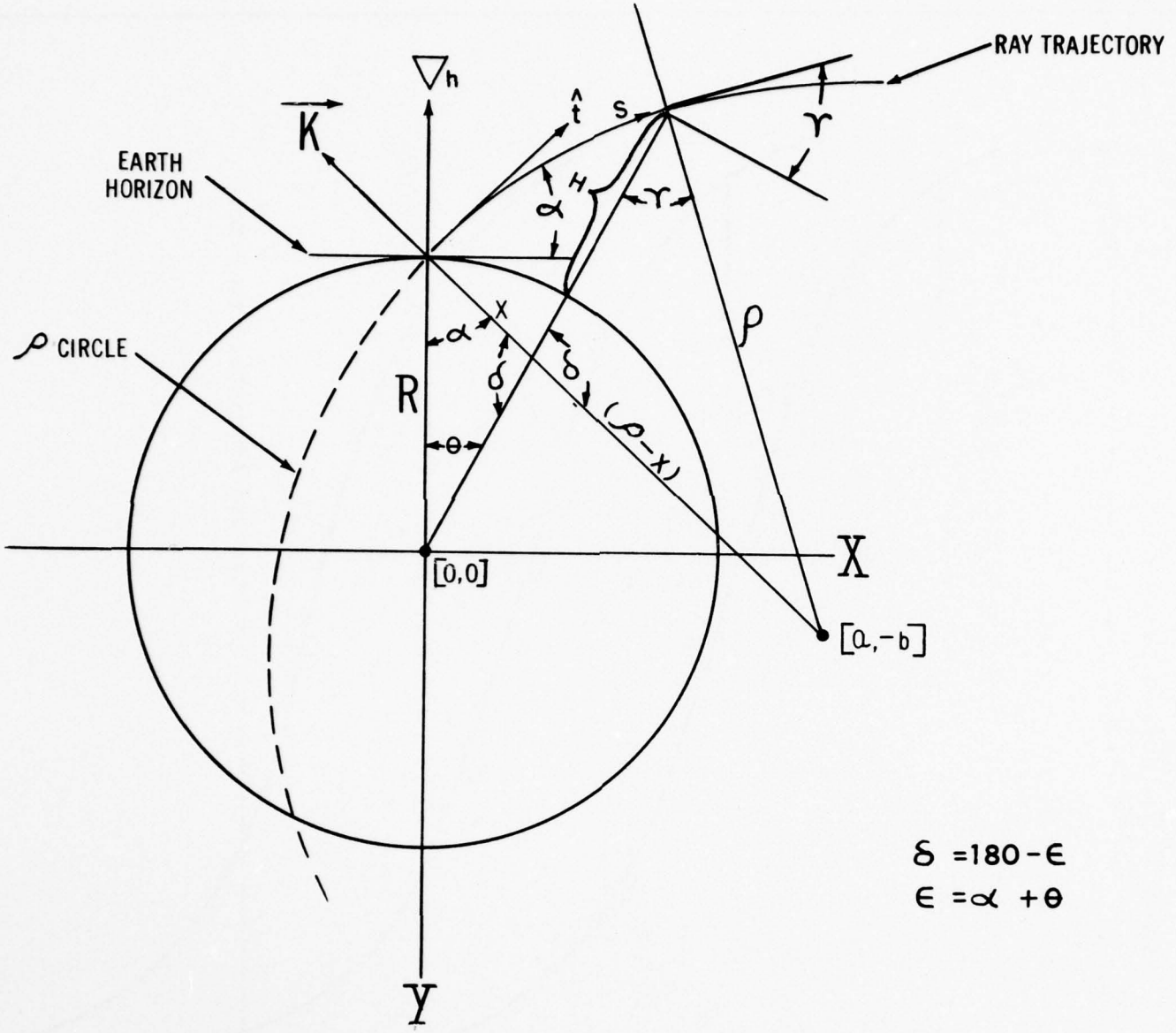

FIGURE 1. GEOMETRY USED TO DERIVE RAY EQUATIONS. (SEE TEXT)

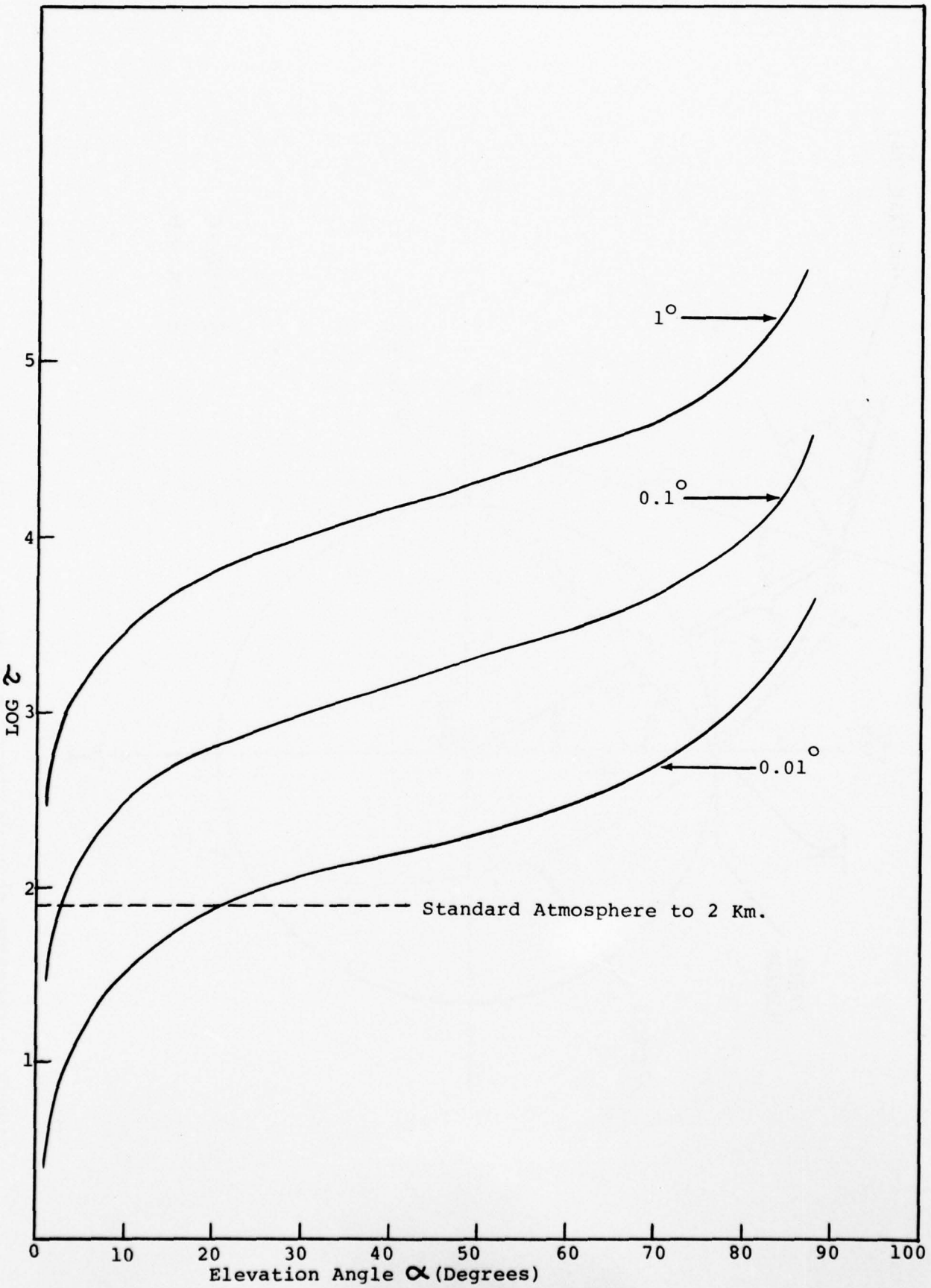

FIGURE 2. LOG τ VERSUS ELEVATION ANGLE (SEE TEXT)

III MICROWAVE AND INFRARED TRANSFER EQUATIONS

In order to arrive at an adequate method for recovering both the temperature and water-vapor profiles, we examine the atmospheric radiation due to water-vapor in the infrared and microwave regions and due to atmospheric oxygen in the microwave region and carbon dioxide in the infrared region. Although the carbon dioxide radiation could be used to determine the temperature profile, it is not considered in this study as it is believed that the infrared sensors at the carbon dioxide radiation wavelength (above 15 microns) are not suitable as those at the water-vapor radiation wavelength (6 to 7 microns). In addition, as the microwave technology is so highly developed, it would appear that it is a more suitable region of the spectrum to use in developing a sensor for temperature and water-vapor. As both carbon dioxide and oxygen can be considered to have a constant mixing ratio up to 2 Km., either could be used to infer the temperature. On balance, for this study, we have chosen to utilize the oxygen radiation for the temperature profile determination.

A. The Radiative Transfer Equation

The amount of radiation emitted by the atmosphere and received by a ground-based radiometer can be determined by the intergration of the transfer equation along the ray path. If we consider the atmosphere to be in local thermodynamic equlibrium (for conditions up to 2 Km of the atmosphere, this is considered to be valid assumption), the radiative transfer equation can be written as[4],

$$\frac{dI(\nu)}{ds} = -k_\nu \left\{ I(\nu) - B_\nu(T) \right\} \qquad (1)$$

where,

$I(\nu)$ = the specific intensity

s = integrating path

k_ν = absorbtion coefficient

$B_\nu(T)$ = Planckian function at ν and T

T = absolute temperature

The solution of (1), evaluated at the ground is,

$$I(\nu) = I_o(\nu) e^{-\tau} + \int_o^\infty B_\nu(T)\, k_\nu(s)\, e^{-\tau} ds \qquad (2)$$

where,

$\tau = \int_o^s k_\nu(s) ds$ is the optical depth

Under the assumption that thereare no sources lying outside of the atmosphere, equation (2) can be written as,

$$I(\nu) = \int_o^\infty B_\nu(T)\, k_\nu(s)\, e^{-\tau(k_\nu, s)} ds \qquad (3)$$

Physically, equation (3) indicates that the received intensity is the sum of each incremental layer emitting as $B_\nu(T) k_\nu ds$ attenuated by the intervening medium by $e^{-\tau}$.

Equation (3) forms the basis for all the inversion techniques that have been used[5] Mathematically, equation (3) does not admit to an analytical solution as the variables involved cannot be described analytically. Consequently, in order to reach a meaningful solution, some constraints, as determined by the physics of the atmosphere, must be imposed.

B. Microwave Radiation Measurements

Because of the simplification that can be applied to equation (3), we treat the microwave case first.

In the microwave region of the spectrum, the Planckian function B can be simplified by the Rayleigh-Jeans approximation($h\nu < kT$) as,

$$B_\nu(T) = 2kT\,\nu^2/c^2 \qquad \text{(frequency units)} \quad (4)$$

The relative error in using (4) is about 0.1% at 60 GHz and 300°K. Substituting (4) into (3) we have that,

$$T_b(\nu) = \int_0^\infty T_\nu(s)\, k_\nu(s)\, e^{-\tau(s)}\, ds \qquad (5)$$

where,

$T_b(\nu)$ = brightness temperature which compares the received radiation from a given direction to that of a blackbody at the temperature T_b

In the troposphere and the microwave region considered(10 to 70 GHz), the principal atmospheric gaseous absorbers and hence emitters are oxygen and uncondensed water vapor. The water vapor absorbtion is due to a pure rotational transition at 22.2 GHz(1.35cm) while the oxygen absorbtion is due to a band of rotational transitions staring at about 53 GHz and extending to 66 GHz. An excellent article on the spectroscopy of the oxygen transitions is to be found in reference (6).

Before equation (5) can be further simplified, the nature and height dependence of the absorption coefficient must be known. Further, it would be desirable to integrate equation (5) to some finite limit rather than to infinity and perferably to 2 KM.

1. Oxygen Microwave Radiation

From the work of reference (6) and (7) a cut-off level can be

established by considering to what level above which the radiation emitted does not make an appreciable contribution to the ground. This has been done for oxygen in terms of the ground absorption coefficient by reference (7). The cut-off level is chosen at the 99% radiation level; however, a more meaningful choice could be made if the exact experimental capabilities of the radiometer in use were known. For example, if the uncertainty in the measurement were .5°K, then the height level corresponding to this value would be chosen. However, the choice of 99% will not change the basic conclusions.

According to reference (7), for a ground absorption coefficient of 12 DB/KM or greater, the cut-off level is about 2 KM. As the ground absorption coefficient for oxygen is about 14 DB/KM[6], we conclude that at least to this level we can utilize a constant absorption coefficient at the center frequency of oxygen band (60 GHz).

To further simplify equation (5), we recast it as ,

$$T_b(\nu) = \int_0^{\tau_c} T_\nu(\tau)\, e^{-\tau} d\tau \qquad (6)$$

as $d\tau$ = kds with T(s) expressed as T(τ) and τ_c is the cut-off optical depth. Equation (6) can be solved analytically if we make the assumption that the T(τ) can be expressed as a Taylor series (this assumption would mean a nearly linear variation of the temperature with τ).

Consequently,

$$T(\tau) = T(0) + \tau \frac{dT}{d\tau} + \frac{\tau^2}{2} \frac{d^2T}{d\tau^2} + \cdots \qquad (7)$$

Substituting into equation (6), it becomes,

$$T_b(\nu) = \int_0^{\tau_c} T_\nu(0) e^{-\tau} d\tau + \frac{dT}{d\tau}\Big|_{\tau=0} \int_0^{\tau_c} \tau e^{-\tau} d\tau + \frac{1}{2}\frac{d^2T}{d\tau^2}\Big|_{\tau=0} \int_0^{\tau_c} \tau^2 e^{-\tau} d\tau + \cdots \quad (8)$$

Since $d\tau = k\,ds$ and integrating the first two terms we have,

$$T_b(\nu) = T_\nu(0)\left(1 - e^{-\tau_c}\right) + \frac{dT}{k\,ds}\Big|_{\tau=0}\left[1 - e^{-\tau_c}(\tau_c + 1)\right] + \frac{1}{2}\frac{d^2T}{k^2 ds^2}\int_0^{\tau_c} \tau^2 e^{-\tau} d\tau \quad (9)$$

Within a given layer having a linear temperature gradient, the second derivative is zero and (9) becomes,

$$T_b(\nu) \cong T_\nu(0)\left(1 - e^{-\tau_c}\right) + \frac{1}{k}\frac{dT}{ds}\Big|_{\tau=0}\left[1 - e^{-\tau_c}(\tau_c + 1)\right] \quad (10)$$

If we designate dT/ds as $\underline{a}$ and choose τ_c to be 5 or greater so that $e^{-\tau_c} < .01$, we have that within a layer characterized by a linear temperature gradient,

$$T_b(\nu) = T_\nu(0) + a/k_o \quad (11)$$

Since we have assumed that $\tau_c \geq 5$ with a constant k_o (up to 2 KM), then $\tau_c = k_o s_c$ defines the upper limit of s. If we include the zenith angle as a parameter then $\tau_c = k_o h_c \sec\theta$. Consequently, the choice of θ and k_o determines the height level, h, that the measurement evaluates. From equation (11), a measurement of T_b that is made for a $\tau_c = 5$, with the ground temperature T_o, will determine the slope $\underline{a}$ of the temperature gradient. Assuming a value of 14 DB/KM for the center frequency of the oxygen transition and converting to nepers/KM (14/4.3429), we obtain that $k_o = 3.224$. Consequently, $h_c \sec\theta = 5/3.224$ or $h_c \sec\theta = 1.55$ KM. If the intial measurement is made near the horizon, say 5^o elevation angle ($\theta = 85^o$), then the effective radiating layer is about 155 meters. It is to be noted that this is not the spatial resol-

ution of the passive method but the layer in which a linear gradient can be ascribed. For most temperature inversions, this is considered adequate for accurately following the temperature gradient. However, if a finer resolution is required, then taking in to account the earth's curvature and working a zero elevation, spatial resolutions on the order of 15 meters could be achieved.

To probe the upper layers, a second measurement is made such that,

$$T_b(\nu) = T(0)\left[1-e^{-\tau_1}\right] + \frac{a_1}{k_0}\left[1-e^{-\tau_1(\tau_1+1)}\right] + e^{-\tau_1}\left[T_1(1-e^{-\tau_2}) + \frac{a_2}{k_0}\left\{1-e^{-\tau_2(\tau_2+1)}\right\}\right] \quad (12)$$

where $\tau_1 + \tau_2 = \tau_c$. As $\underline{a}_1$ has been determined from the initial measurement, a τ_1 can be calculated with $T_1 = T_o + \underline{a}_1 h_c$ of the first measurement. From equation (12), the $\underline{a}_2$ is determined. Again, the combination of k_o and θ is used so that $\tau_c = \tau_1 + \tau_2$ yielding the $\underline{a}$ in the second layer. The process is continued until the entire 2 KM is probed. From the foregoing analysis it is seen that for a single gradient, only one measurement is necessary. For two gradients, two measurements are required and so on. Based on the fact that 10 changes in slope is about the maximum number of changes that occur, no more than 10 measurements are necessary to characterize the temperature distribution of the first 2KM of the atmosphere. In general then, the n^{th} measurement can be written as,

$$T_n = T_o(1-e^{-\tau_1}) + \frac{a_1}{k_0}\left[1-e^{-\tau_1(\tau_1+1)}\right] + \sum_{i=1}^{i=n} e^{-\tau_i}\left[T_i(1-e^{-\tau_{i+1}}) + a_{i+1}\left\{1-e^{-\tau_{i+1}(\tau_{i+1}+1)}\right\}\right] \quad (13)$$

where $\sum_{i=1}^{n} \tau_i = 5$.

The expected spatial resolution will be determined by the measurement errors and the number of meaurements made but has the potential, at least in principal, of at least 15 meters.

2. Water Vapor Microwave Radiation

The behavior of the water vapor attenuation in the microwave region near the resonance line (1.35 cm.) is remarkable as it can be shown [8] that the attenuation is independent of pressure and depends only on the fraction of water vapor present (i.e. mixing ratio). However, even under humid conditions of the atmosphere (i.e. over ocean areas), the absorption coefficient is not large enough ($\sim$.66 DB/KM for ρ_w = 2lg/M^3 at 1.35 cm.) to be apply the method used for oxygen. Although the gross water vapor structure could be determined, for a multi-jagged variation where high spatial resolution is required, it is not the method of choice. Consequently, it is felt that the water vapor structure can best be determined by utilizing the infrared water band at 6.5μ.

C. Infrared Water Vapor Radiation

In the infrared portion of the spectrum, the Rayleigh-Jeans approximation cannot be used and equation (3) must be used as is. Due to the fact that the water vapor attenuation does not follow the Lambert law of exponential absorption [9], it is necessary to cast equation (3) in a slightly different form. If the transmission through a layer is t, then dt/ds expresses both the emission and attentuation from the layer. Consequently,

$$dI(\nu) = B_\nu(s)\, dt \tag{14}$$

For a layer of constant B(s), then the intensity received at the ground due to a layer at s is just,

$$I_s(\nu) = B_\nu(s)\,(t_1 - t_2) \tag{15}$$

where,

t_1 = transmission from the bottom of the layer

t_2 = transmission from the top of the layer

The measured intensity is just the summation from each layer. Then,

$$I(\nu) = B_\nu(0)(t_0 - t_1) + B_\nu(1)(t_1 - t_2) + \cdots \quad (16)$$

where,

$B_\nu(0)$ = Planckian function for the ground temeperature

t_o = transmission at the ground level equal to 1

t_1 = transmission from the top of the ground layer

t_2 = transmission from the top of the second layer

$B_\nu(1)$ = Planckian function for the temperature of layer 2

Before proceeding to derive the equations that determine the spatial resolution potential of the infrared radiation, an expression relating the transmission to ρ_w is necessary. Although the transmission cannot be expressed through an exponential attenuation coefficient, it can be approximated by[7],

$$t \cong e^{-.64\left(\frac{w}{w_o}\right)^{.55}} \quad (17)$$

where,

w = optical thickness of water vapor in preciptable cms.

w_o = optical thickness necessary to yield 50% transmission

In addition, w_o is a function of wavelength and can be expressed as $w_o^{.55} \cong .337/K(\lambda)$[9]. The values of $K(\lambda)$ have been tabulated by Green and Griggs[9]. Substituting the expression for w_o into equation (17) we obtain,

$$t \cong e^{-1.90\, w^{.55} K(\lambda)} \quad (18)$$

Now it can be shown that the equivalent optical thickness of water vapor in terms of pressure and temperature of the atmosphere can be written as[9]

$$W = \int_{S_1}^{S_2} \frac{P}{P_o}\left(\frac{T_o}{T}\right)^{1/2} \rho_w \, ds \tag{19}$$

where,

P = pressure in atmospheres

P_o = ground or local pressure

T = absolute temperature

T_o = ground or local temperature

However, ρ_w can be written as,

$$\rho_w = \frac{10^{-3} m M P}{RT} \tag{20}$$

where,

m = mixing ratio (g/Kg)

R = gas constant

M = molecular weight of air

Substituting (20) into (19), we have that,

$$W = \frac{10^{-3} M T_o}{R P_o} \int_{S_1}^{S_2} \frac{P^2}{T^{3/2}} m \, ds \tag{21}$$

Within an isothermal and isobaric layer, this becomes,

$$W(s) = \frac{10^{-3} M T_o^{1/2} P^2(s) m(s) \Delta s}{R P_o T^{3/2}(s)} \tag{22}$$

Consequently,

$$m(s)\Delta s = \frac{10^3 R P_o T^{3/2}}{M T_o^{1/2} P^2} \tag{23}$$

Inserting the appropriate constants, we have that,

$$m(s)\Delta s = \frac{82.057 \times 10^3 P_o T^{3/2} w(\Delta s)}{28.97 \quad P^2 T_o^{1/2}}$$

$$m(s)\Delta s = 2.832 \times 10^3 \frac{P_o T^{3/2} w(\Delta s)}{P^2 \quad T_o^{1/2}} \tag{24}$$

As T (s) is known (oxygen measurement) and P(s) does not vary much and is reasonably predictable and with P_o and T_o measured quantities, a measurement of $w(\Delta s)$ through equation (18) determines the product $m(s)\Delta s$.

Returning to equation (16), it is necessary to limit the intensity summation similar to way a cut-off τ was used in the oxygen measurement. The limit of the summation process will depend on the error measurement on I. For the purposes of this report, we will assume that the smallest variation is .01 although the actual value will depend on the experimental capabilities of the radiometer. As B(o) and t_1 are known from ground base measurements, we will choose a measurement at λ_1 that produces a $t_1 = .02$. This in effect eliminates any term beyond B(1) since $t_1 > t_2 > t_3$ and assures that $t_2 - t_3 < .01$. Rewritting equation (16) at λ_1 we have that,

$$I(\lambda_1) = B_{\lambda_1}(o)(1 - t_1) + B_{\lambda_1}(1)(t_1 - t_2) \tag{25}$$

or,

$$I(\lambda_1) = .98\, B_{\lambda_1}(o) + B_{\lambda_1}(1)[.02 - t_2] \tag{26}$$

The single measurement yields t_2. In order to preclude the possibilty that t_2 is also equal to .02, we will assume that the mixing ratio never gets below 40% humidity at any level to 2 KM.

This will correspond to a lower limit of about 2 g/Kg. This assumption is considered valid over the ocean.

The choice of $t_1 = .02$ and the ground measured value of m_1, produces a Δs at a given wavelength through equation (24). With the value of t_2 obtained from equation (26) and the derived value Δs obtained from equation (24), the value of m_2 is determined.

The next measurement would be made at the λ_2 that produces a $t_1 > .02$ (calculated from Δs and m_1) and the t_2 calculated from Δs and m_2. Consequently,

$$I(\lambda_2) = B_{\lambda_2}(0)[1 - t_1] + B_{\lambda_2}(1)[t_1 - t_2] + B_{\lambda_3}(2)[t_2 - t_3] \quad (27)$$

From this measurement, t_3 is determined from which m_3 can be calculated using the same value of Δs from t_1 and t_2. This process is continued until the entire 2KM of the atmosphere is probed. As can be seen from this process, the spatial resolution will be determined by the number of measurements that are made and the limitations of the capabilities of the radiometer.

In order to assess, the potential spatial resolution of the passive method, we compute the spatial resolution that could be achieved from a humid ground layer. From equation (24) using $P_o = 1$ atmosphere and $T_o = 290^{\circ}K$ and $m_1 = 10$ g/Kg,

$$\Delta S = 8.212 \times 10^4 w \quad (cm) \quad (28)$$

From equation (18), if this layer is to produce a $t_1 = .02$, then for $K(\lambda) = 13$ (peak absorption coefficient for water vapor occurring at 6.60μ) yields a $w_1 = .035$ preciptable cms. Consequently, $\Delta S = 2874$ cm or 28.7 meters. However, since $\Delta s = \Delta h \sec\theta$, the resolution is increased at large zenith angles so that in principal, resolutions on

on the order of 2 to 3 meters ($\theta = 85^{o}$) are possible. However, as mentioned previously, this increases the number of measurements that must be made to probe the 2 Km. of the atmosphere. Additonally, since the absorption coefficient of water-vapor in the infrared has a wide latitude (13 to 10^{-3}) and in conjunction with the zenith angle, coarse or fine resolution measurements could be achieved.

Although the microwave radiation from atmospheric oxygen can be used to determine the temperature profile with a potential resolution of about 15 meters, it is seen that the microwave radiation from atmospheric water-vapor does not provide an attenuation coefficient high enough from which a high resolution profile could be extracted. Consequently, it is necessary to utilize the infrared radiation from atmospheric water-vapor to extract a water-vapor profile.

IV. MICROWAVE AND INFRARED SYSTEM SENSITIVITY AND RESOLUTION

In this section we analyze the expected system sensitivity and resolution. We assume that the temperature profile has been determined by the microwave method and examine first how many meaningful measurements can be made using the infrared water-vapor absorption band and what spatial resolution does this represent.

As we have shown by the previous anlysis, the answer is complex and dependent on the profile and the existing ground conditions. In addition, the spatial resolution, as will be shown, becomes non-lnear which complicates arriving at a meaningful answer. Although, using a spatial technique produces a non-linear spatial resolution, the passive method is still a viable method, as it will be shown in section VI that employing a gradient technique removes most of the non-linearity. However, for this analysis we show how the infrared radiation from water-vapor will produce a non-linear response in terms of spatial resolution.

A. Determination of Radiometer Noise

Before pursuing this analysis, it is necessary to consider the limitation due to noise of an infrared radiometer. A typical radiometer consists of a Cassegrain-type optical system which focusses the radiation onto a plane which includes a field-defining aperture. After mechanical chopping of the image, the radiation is relayed optically to an infrared detector. Solid state electronics amplify, demodulate and filter the signal produced by the detector producing an

output voltage that is an accurate measure of the received radiation. In addition, detectors are interchangeable and specific filters are easily interchanged.

The radiometric sensitivity given in terms of noise equivalent radiance (NER) is computed from,

$$NER = \frac{A_D^{1/2} (\Delta f)^{1/2}}{D^* t A \omega} \qquad (1)$$

where, A_D = area of the detector
Δf = output noise bandwidth ($\sim$ 1Hz)
A = area if collecting optics
D^* = detector figure of merit ($cm(Hz)^{\frac{1}{2}}$/watts)
t = transmission of the optical system
ω = solid angle field of view (steradians)

For a typical research radiometer (e.g. Barnes spectral-master, Models 12-550 or 12-660), we have that,

A_D = .1mm x .5mm ($\sim 2.5 \times 10^{-3}$ cm^2)

D^* = 5×10^8 (immersed Bolometer at 325^oK)

t = .4

A = 90 cm^2

ω = 10^{-4} steradians

Consequently, for this system, NER $\cong 10^{-9}$ watts/$cm^2 \omega$. We define B(the blackbody radiance) in terms of watts/$cm^2 \omega$ $cm_{\Delta\lambda}$ where $cm_{\Delta\lambda}$ means centimeter wavelength interval. If we limit the radiation received by the radiometer at particular height in the atmosphere, we must have that,

$$B_{max} t \Delta\lambda = NER \qquad (2)$$

where,

t = transmission of radiation to the ground from some level of the atmosphere

B_{max} = highest blackbody radiance seen by the radiometer (i.e. highest temperature)

$\Delta\lambda$ = wavelength bandpass of the radiometer

If we further restrict the radiometer to .1μ wavelength interval at 7μ (i.e. $\Delta\lambda = 10^{-5}$ cm) we have that,

$$t = \frac{10^{-4}}{B_{max}} \tag{3}$$

For a normal lapse rate, B_{max} is the B for the ground temperature. At 25°C, $B(25^{o}C) = B_{max}$ is 7.16 watts/cm$^2\omega$ $cm_{\Delta\lambda}$ at 7μ . Consequently, $t \cong 10^{-5}$. This indicates that the radiometer sensitivity is on the order of $10^{-5}B_{max}$. However, this is necessarily too sensitive and we assume that by a suitable change of one of the parameters in equation (1), we can degrade the sensitivity to $10^{-4}B_{max}$. We will call this the noise equivalent blackbody radiance (NEB). Consequently, any signal received can be written as,

$$\text{Signal} = \text{SNR}\ 10^{-4}B_{max} \tag{4}$$

where, SNR is the signal to noise ratio.

B. Determination of Sensitivity

According to section III, part C, the measured intensity or effective B is given by,

$$I/\Delta\lambda = B_1(1-t_1) + B_2(t_1-t_2) + \cdots B_n(t_n-t_{n+1}) \tag{5}$$

We rewrite equation (5) as,

$$I/\Delta\lambda - B_1(1-t_1) = B_2(t_1-t_2) + \Sigma_u \quad (6)$$

where, Σ_u= summation of all the upper layers. If t_2 is chosen such that the $\Sigma_u \cong 0$ (i.e. $t_2 = 10^{-4}$) then,

$$I/\Delta\lambda - B_1(1-t_1) = B_2(t_1-t_2) \quad (7)$$

The magnitude of the signal is given by equation (4). Consequently,

$$B_2(t_1-t_2) = SNR\ 10^{-4}B_{max} \quad (8)$$

or dividing by t_2 we have that,

$$SNR = \frac{t_2\ B_2}{10^{-4}B_{max}}(\ t_1/t_2 - 1) \quad (9)$$

since $t_2 = 10^{-4}$,

$$SNR = \frac{B_2}{B_{max}}(\ t_1/t_2 - 1) \quad (10)$$

i.e., independent of t_2.

Before proceeding, we require a known temperature profile. As a first case, we choose a linear gradient starting with 298°K at the ground and decreasing to 288°K at 2 KM. For this case, the minimum SNR becomes,

$$(SNR)_{min} = \frac{B(288)}{B(298)}(t_1/t_2 - 1) \quad (11)$$

or,

$$(SNR)_{min} = .79(t_1/t_2 - 1) \quad (12)$$

From section III,part C, we showed that,

$$t = e^{-1.90K\sec\theta^{.55}w^{.55}} \quad (13)$$

where θ = the zenith angle. Hence,

$$t_1/t_2 = e^{-1.90K\sec\theta^{.55}(w_1^{.55} - w_2^{.55})} \tag{14}$$

We will call $K\sec\theta^{.55}$, Φ , and write that,

$$t_1/t_2 = e^{-1.90\,\Phi\,(w_1^{.55} - w_2^{.55})} \tag{15}$$

In order for equation (7) to be valid, we also must have that,

$$t_2 = 10^{-4} = e^{-1.90\,\Phi\,w_2^{.55}} \tag{16}$$

or,

$$\Phi = \frac{\ln\,(10^{-4})}{-1.90\,w_2^{.55}} \tag{17}$$

Consequently, a given W_2 defines Φ . This indicates that any combination of K and sec $\theta^{.55}$ produces a given Φ . For the purposes of this analysis we will assume that sec θ varies from 1 to 7 corresponding to $\theta = 0^{\circ}$ to $\theta = 82^{\circ}$. For $\theta = 82^{\circ}$, we can still assume a flat earth. The variation of K goes from a peak of about 13 at 6.70 μ and we chose a lower limit of K=1 at about 7.50 μ . Consequently Φ can vary from 1 to about 38.

A plot of Φ versus W_2 is shown in figure 3 according to equation (17). On the same curve is plotted the expected SNR for a given $(w_1^{.55} - w_2^{.55}) = \delta$. This was computed by combining (12)and (15). These curves indicate the expected SNR for a given difference of w in a two layer system.

It is to be noted that in this method, we are always working in a wavelength region where the radiation is optically black. Consequently, the measurements in intensity at different Φ , will only reflect the changing B or the effective $\langle B \rangle$.

Before proceeding, we now require the ground value of the water vapor

density ρ_w or its equivalent the mixing ratio. In addition, we choose the spatial resolution required. The combination of measured ρ_w and ΔH produces w_1, the optical depth of ρ_w at ΔH. Consequently, for a given Φ, the term $B_1 (1-t_1)$ in equation (7) is defined which in turn defines $B_2 (t_1-t_2)$.

The determination of Φ to be used to calculate $B_2 (t_1-t_2)$ in equation (7) is obtained as follows:

The ρ_w or w at any given increment ΔH must lie between w_s (w at saturation) and some limiting value, say 20% humidity or .2 w_s. This is indicated in figure 4. Plotted between them is the w for the linear temperature profile given above and an exponential water vapor profile starting at 20 g/M^3 at the ground and ending at 10 g/M^3 at 2 KM. This w curve was calculated at 50 meter increments. We use this curve as a model to the determine the spatial resolution.

At a ΔH = 50 meters and a ρ_w = 20 g/M^3, the w at 50 meters is .10 pr. cm. If we continue at 50 meter increments, the value of w_2 at 100 meters for a saturated layer is .3 pr. cm. while for a 20% humidity it is .12 pr. cm.. Hence expect that the measured value between 50 and 100 meters should fall between the values computed as follows:

$$w_s(50 \text{ to } 100) = w_s(100) - w_s(50) = (.3 - .15) = .15$$
$$w_{20}(50 \text{ to } 100) = w_{20}(100) - w_{20}(50) = (.06 - .03) = .03$$

Consequently for the 50 to the 100 meter layer,

$$w_2 = .1\begin{cases} + .15 \\ + .03 \end{cases} = \begin{matrix} .25 \\ .13 \end{matrix}$$

Referring to the w_2 curve of figure 3, this produces a range of Φ = 15.0 to Φ = 10.2. The measured value of $I/\Delta\lambda - B_1(1 - t_1)$ can be obtained as Φ is scanned from 15.0 to 10.2. Each value of Φ will produce a signal at a given SNR. However, the $-\delta$ values for saturation and 20% humidity are .184 and .043 respectively. At $-\delta$ = .184 at Φ = 10.2,

the SNR is 27 while at $-\delta = .043$ and $\Phi = 15.0$, the SNR is 2. Since the actual value of w is .20, this would produce an SNR of about 14 at $\Phi = 11.8$. Scanning the Φ from 15.0 to 10.2 would produce the SNR that is consistent with the actual w_2.

Once w_2 is determined, the process is continued for the third layer. Now t_1 represents the transmission to the ground from the top of the first two layers and the t_2 from the top of the third layer. In each layer, the limits of saturation and 20% humidity determines the range of Φ that is to be scanned and the SNR obtained that is consistent with the $-\delta$ for each Φ results in the value of w for that layer.

To obtain a measure of the expected resolution for this process and the number of measurements that can be made, we examine the process in reverse and calculate the minimum thickness of the atmosphere that is necessary that will produce a SNR = 1, starting from the top of the 2 KM layer using the calculated w curve for the model ρ profile. This is computed from,

$$\delta_{SNR=1} = \frac{\ln(2.27)}{-1.90} \tag{18}$$

and from,

$$w_1 = (\delta + w_2^{.55})^{1.818} \tag{19}$$

The results are shown in Table I. From this we conclude that for a nearly satured ρ_w profile, neglecting the first 100 meters, we can make about 17 measurements. However, the spatial resolution is non-linear, being fine at the bottom of the atmosphere and becoming coarser as higher layers are probed. As the course of radio waves are affected by w rather than ρ_w, we believe that the coarse resolution at the top layers is not a serious restriction of the method.

TABLE I*

H (Meters)	w_2	Φ	δ	$w_1^{.55}$	$w_1^{.55}$
2000	2.96	2.70	-.160	1.66	2.51
1600	2.51	2.92	-.148	1.51	2.12
1300	2.12	3.20	-.135	1.38	1.79
1100	1.79	3.50	-.123	1.25	1.51
850	1.51	3.80	-.114	1.14	1.27
700	1.27	4.25	-.102	1.04	1.07
580	1.07	4.70	-.092	.946	.904
480	.904	5.10	-.085	.861	.762
400	.762	5.60	-.077	.784	.643
330	.643	6.20	-.0696	.715	.543
280	.543	6.70	-.0644	.650	.457
230	.457	7.40	-.0583	.592	.385
200	.385	8.20	-.0526	.539	.325
170	.325	9.00	-.0479	.491	.274
140	.274	9.90	-.0436	.447	.231
120	.231	10.80	-.0400	.407	.195
100	.195				

*Tabulation of W values for the model profile used to determine the expected resolution (see text above).

C. Microwave System

The microwave radiometer spatial resolution and temperature sensitivity is a function of the requisite parameters for a viable probe. For example, as the normal temperature gradient of the atmosphere is about -6.5 ^{o}K/Km (-.0065 ^{o}K/Km) and a spatial resolution of 50 meters is required, then the microwave radiometer should be able to resolve about .3^{o}K.

The temperature sensitivity of the radiometer can be expressed as,

$$T_{MIN} = \frac{C(N-1)}{\sqrt{Bt}} T_o = \frac{C T_e}{\sqrt{Bt}} \qquad (20)$$

where,

T_{min} = root-mean square temperature fluctuation (minimum detectable temperature)
N = noise figure
t = integration time
T_o = ambient temperature
C = constant between 1.5 and 2 (depends on mode of operation)
T_e = excess receiver noise temperature

For a sytem operating at 60 GHz (oxygen band), with an IF bandpass of 20 MHz (typical), the T_{min} is a function of the excess receiver noise. Assuming an integration time of 10 sec. and a T_o of 290^{o}K with C = 2, we have that,

System Noise (DB)	Sensitivity (^{o}K)
20	4
17	2
10	.37
8	.22
5	.09

Consequently, a system noise of about 10 DB is necessary to meet this requirement.

In terms of the spatial resolution of the radiometer, the gain of the antenna used determines the area over which the received energy is integrated. Hence the beamwidth is a measure of the resolving power of the antenna. For a paraboloid antenna, the effective area, A, is about 55% of the physical area. A general relation of the antenna gain G, is given by,

$$G = \frac{4\pi A}{\lambda^2} \tag{21}$$

At 60 GHz and a diameter of the antenna of 1 foot, the gain (55% efficiency) is about 40 DB. The angular resolution of the antenna is given by,

$$\Theta \cong \frac{\lambda}{D_o} \tag{22}$$

where λ = wavelength of the received radiation(.5cm)
D_o = effective diameter of the antenna ($D_o = D\sqrt{.55}$).

Consequently, the angular resolution is about .022 radians($\sim 1.3^{o}$). At 2 KM (limit of the temperature probe), this represents a physical area of about 44 meters in diameter which is consistent with the assumed temperature spatial resolution requirement.

In practice, the antenna gain is determined empirically. For

the stated requirements, a 1 foot diameter antenna with a noise figure of 10 DB, appears to meet the needs of a viable probe.

Both system cost and complexity cannot be determined but must be evaluated when the results of the error propagation analysis is made.

As microwave radiometry is a well developed technology, it is concluded that a properly designed system can adequately meet any necessary requirements.

D. Infrared System

The spatial resolution of an infrared system utilizing a Cassegranian telescope as the receiver more than adequately meets the spatial resolution requirements (due to much shorter wavelength $\sim 6.5\mu$). The sensitivity of the system to water vapor concentration changes will be a function of the limits imposed by the error analysis, the requisite requirements of the probe and the ability of the radiometer to measure intensity changes.

The noise equivalent radiance (NER) of the radiometer can be computed from,

$$NER = \frac{\alpha^{1/2} (\Delta f)^{1/2}}{D^* e A \omega} \qquad (23)$$

where, α = detector area
Δf = output noise bandwidth
A = area of the collecting aperture
ω = solid angle field of view
D* = detector figure of merit
e = transmission of the optical system

For a typical system, we have that α = .12mm x .48mm, Δf = 1 Hz, A = 8.5 cm^2, ω = .0012 sr, D* = 10^8 $cm(Hz)^{\frac{1}{2}}$/watt and e = .4. Using these values NER = 6x 10^{-8} watts/cm^2-sr.

To translate this into an equivalent sensitivity for water vapor concentration, we proceed as follows:

For a given radiating layer, the emitted intensity is $I_L = B_L(t_1 - t_2)$ where the symbols were defined in progress report #2. As t_2 is the transmission from the top of the layer to the ground, it can be expressed as $t_2 = t_L t_1$ where t_L is the transmission through the layer. Then $I_L = (t_1 - t_L t_1)B_L$. A change in the emitted intensity due to a change in the transmission of the layer from a change in the water vapor concentration and assuming a constant temperature in the layer results in $\Delta I_L = -t_1 \Delta t_L$. As it was shown in section III, part C that t_L is related to the optical thickness w through,

$$t = e^{-1.90\,K(\lambda)\,w^{.55}} \tag{24}$$

a change in t_L due to a change in w becomes,

$$\Delta t_L = -1.90\,K(\lambda)\,e^{-1.90K(\lambda)w^{.55}}(.55)w^{-.45}\Delta w \tag{25}$$

In terms of the mixing ratio m, the w is in turn related to m through $m\,\Delta s \cong 8.50 \times 10^{5} w$, assuming a P_o = 1 atmosphere and a T_o = 300°K. Using a $K(\lambda)$ = 13 (peak of the water vapor absorbtion) and substituting into equation (25) we obtain that,

$$\Delta m = \frac{8.50 \times 10^{5} w^{.45} \Delta I_L}{\Delta s\, t_1 B_L (13.6) e^{-24.70 w^{.55}}} \tag{26}$$

If we assume a spatial resolution (in depth) of 50 meters as before and a typical value of w = .01 pr. cm., with t_1 nearly 1, we have that,

$$\Delta m \cong \frac{10\,\Delta I_L}{B_L} \tag{27}$$

We equate the ΔI_L to the sensitivity of the radiometer and obtain that the sensitivity in terms of the mixing ratio is,

$$\Delta m \cong \frac{10\,NER}{B_L} \tag{28}$$

The B_L is the blackbody radiation at the bandpass and wavelength of the radiometer. At 6.5 microns with T = 300°K and assuming a bandpass of 0.1 microns for the radiometer, $B_L = 4 \times 10^{-4}$ watts/cm^2-steradian. Substituting the calculated value of the NER, we obtain that,

$$\Delta m \cong 10^{-2} \text{ g/Kg} \tag{29}$$

Although this is an approximate value, it indicates that, potentially that the method has a sensitivity that exceeds any reasonable requirements for a probe.

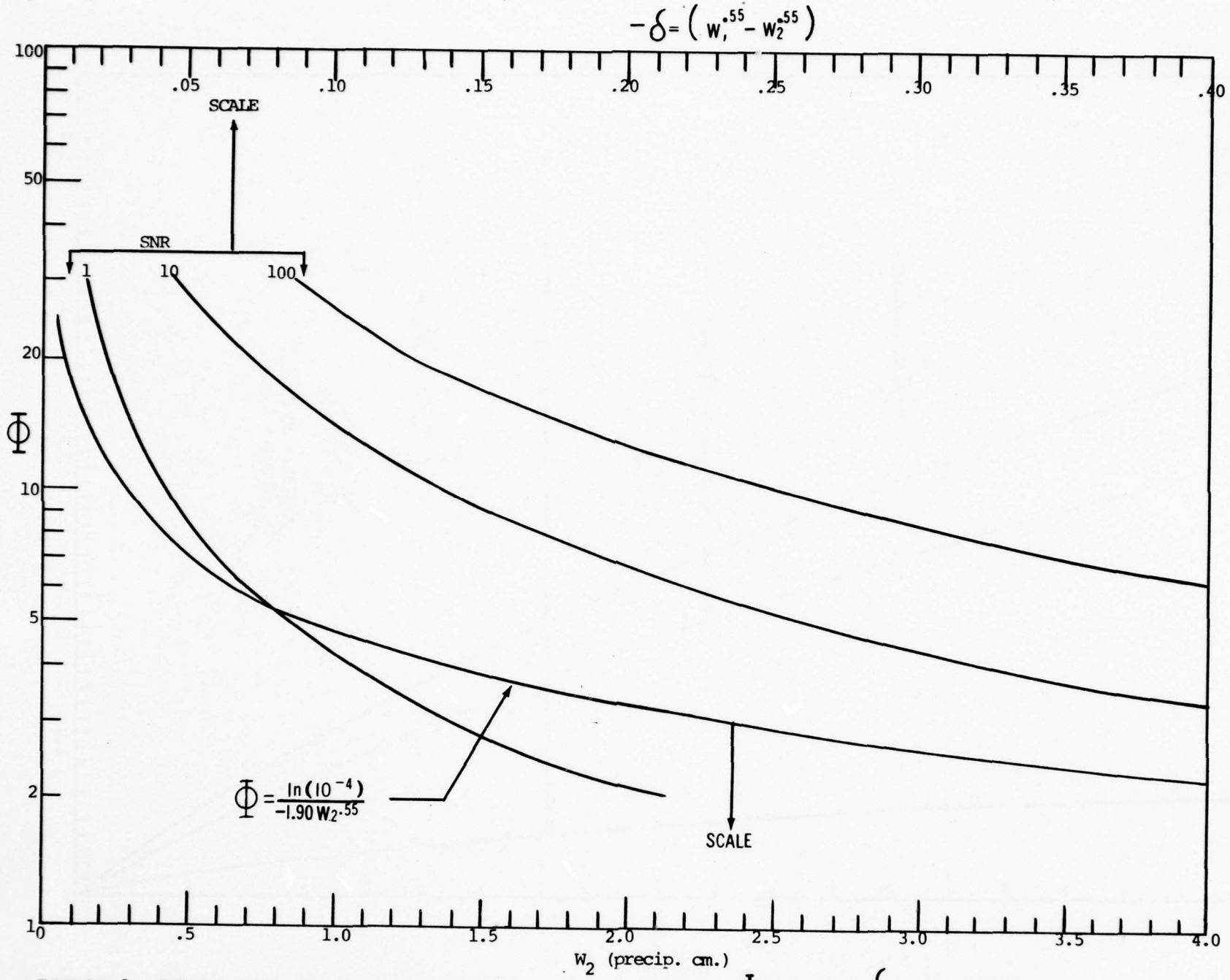

FIGURE 3. CURVES USED TO DETERMINE THE SNR FOR A GIVEN W_2, Φ AND δ. (SEE TEXT)

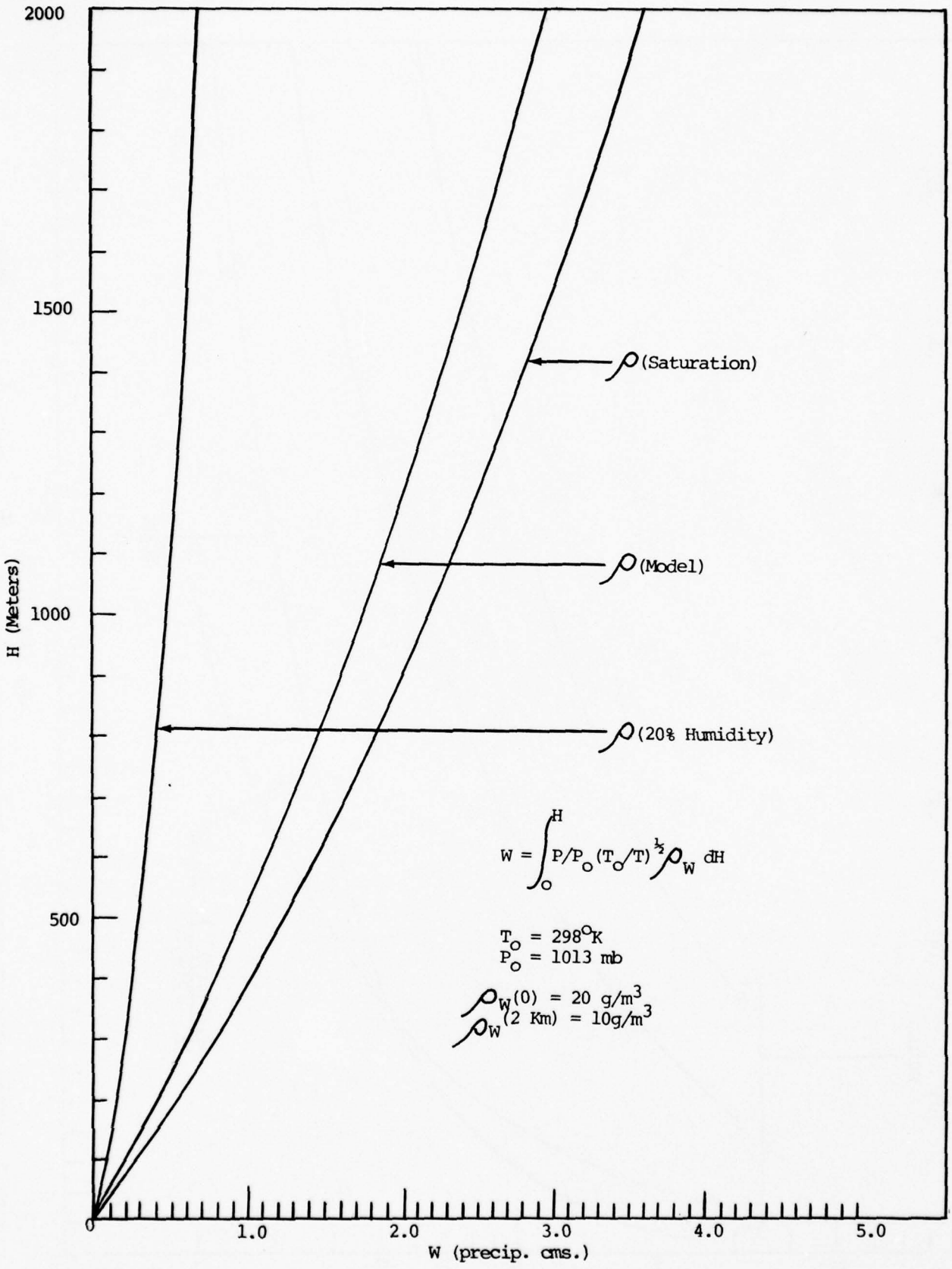

FIGURE 4. CALCULATED VALUES OF W FOR THREE ρ PROFILES VERSUS H (SEE TEXT)

V. EFFECT OF VISIBILITY ON PASSIVE PROBES

In order for a probe for water-vapor and temperature to be useful, whether active or passive, it must be capable of operating under varying degrees of visibility. The effect of visual range (i.e. visibility) of 1 to 10 Km on both the infrared and microwave passive methods is evaluated in this section.

As visual range is a subjective parameter while the proposed passive methods are objective measurements, a criterion must be established to relate the two. Visual range, as defined, depends on the ability of an observer (i.e. the "standard" eye) to distinguish an object from it's background light (contrast). In its most general form, the reduction in contrast for an observer, under different sky brightness conditions is given by[11],

$$B_R - B_R' = (B_o - B_o')e^{-\sigma_o \bar{R}} \tag{1}$$

where, B_o and B_o' are the inherent luminances of the object and background respectively, B_R and B_R' are the reduction in luminance at the distance R of the object and background respectively, σ_o the extinction coefficient for a homogeneous layer of the atmosphere and $\bar{R}$, the optical range; defined as the equivalent horizontal distance which produces the same attentuation as the actual range R. Calling the inherent contrast C_o, we have that,

$$C_o = \frac{B_o - B_o'}{B_o'} \tag{2}$$

and the apparent contrast C_R as,

$$C_R = \frac{B_R - B_R'}{B_R'} \tag{3}$$

we have that equation (1) can be written as,

$$C_R = C_o (B_o'/B_R') e^{-\sigma_o \overline{R}} \tag{4}$$

Due to the fact that the eye contrast threshold ϵ, depends on the angular subtense of the object and that for a particular object this in turn depends on the range and that the resulting contrast depends on the luminance of the background, equation (4) admits to a range of values. Nomograms for a variety of luminance values and object sizes are available to determine visual range for a given set of conditions [12]. However, for the purposes of evaluating the passive methods, we utilize equation (4) for the case of an object seen against the horizon sky. If C_o is greater than ϵ, then equation (4) becomes,

$$\epsilon = C_o e^{-\sigma_o V} \tag{5}$$

where, V = visual range

ϵ = luminal contrast.

As we are concerned with the evaluation of σ_o, we assume a black object (C_o = -1) and equation (5) can be rearranged to,

$$V = \frac{1}{\sigma_o} \ln\left|\left(\frac{1}{\epsilon}\right)\right| \tag{6}$$

Before σ_o can be evaluated, a value for ϵ must be assigned. If we use the meteorological range as the criterion for visibility, then ϵ = .02 and equation (6) can be written as,

$$\sigma_o = 3.912 / V_2 \qquad (7)$$

where, V_2 = the meteorological range. Consequently, a meteorological range of 1 to 10 KM produces a value of σ_o of 3.912 KM^{-1} to .3912 KM^{-1}. This range of extinction coefficients must now be related to some power law with wavelength in order to assess its' effect in the infrared and the microwave regions.

The most general form of σ can be written as,

$$\sigma = c_1 \lambda^n + c_2 \lambda^{-4} \qquad (8)$$

where, c_1 and c_2 are constants, λ the wavelength and the second term reflects the Rayleigh extinction coefficient for pure air.

As for pure dry air, the visual range is over 350 KM [11], we are justified in considering only the first term in equation (8) when dealing with a visual range of 1 to 10 KM. Consequently, $\sigma \cong c_1 \lambda^n$ where the exponent n must be evaluated on the basis of the type of scattering and absorbing particle involved.

In order to evaluate the exponent n, recourse is made to the Mie theory of scattering in which the cross-section for extinction can be wriiten as,

$$\sigma = N \pi r^2 K \qquad (9)$$

where, N = number of particles cm^{-3}

r = radius of the particle

K = efficiency for extinction

K is ratio of the extinction coefficient to the geometric cross-section of the particle. From the Mie theory, the K is a function of α, the size parameter, equal to $2\pi r/\lambda$. For a dielectric sphere (i.e. a water drop) with a refractive index of 1.33, K is about 4

when $\alpha = 1$. Above $\alpha = 1$, the K fluctuates about K = 2 and approaches 2 for large values of α and eventually approaches 1 in the geometric region. From equation (8) and equation (9) we can write,

$$N\pi r^2 K = C_1 (r/\lambda)^{-n} \tag{10}$$

Taking the log of equation (10) yields,

$$\log K + \log(N\pi r^2) = \log C_1 - n \log (r/\lambda) \tag{11}$$

Consequently, for a given value of r and λ, K can be calculated from Mie theory for a given refractive index, allowing the determination of n. This has been done for water spheres (m = 1.33) and completely absorbing spheres ($m = \infty$) by reference (11). For water spheres, the value of n = -4 for very small spheres (Rayleigh extinction), becomes n = -2 for r about $\lambda/2$ and n = 0 for $r = \lambda$. It then becomes temporarily positive and oscillates about zero as r/λ increases. For completely absorbing spheres, the transition from n = -4 to n = 0 occurs at $r/\lambda = .2$. Although the Mie theory predicts an oscillating value for n for large values of α, these effects are not observed as atmospheric aerosols are mainly polydisperse resulting in a dampning of the oscillation in n. Consequently, depending on the value of m, a critical value of r is reached where the extinction becomes independent of wavelength.

Accordingly, the extinction coefficient for atmospheric aerosols can be used to determine the value of n. Empirically it has been found that[13],

$$n \cong 5.85 \times 10^{-2} V_2^{1/3} \quad (V_2 \text{ in meters}) \tag{12}$$

Although this equation has been evaluated for a range of 1 to 5 KM,

for the purposes of this calculation, we will assume that it is also valid up to 10 KM. Combining equation (7) with (9) we have that,

$$\langle N \rangle = \frac{3.912}{V_2 \pi \langle r \rangle^2 K(\alpha)} \qquad (13)$$

where the brackets indicate the average value. As equation (12) permits a determination of n which in turn defines both $K(\alpha)$ and r, (using and average value of $\lambda = .5\mu$ for the visible), permits and estimation of $\langle N \rangle$ from equation (13).

Assuming that water droplets produce the reduction in visibility, (reasonable assumption for open ocean areas), a range of 1 KM produces an $\langle r \rangle = .43\mu$ and $\langle N \rangle \cong 2.2 \times 10^9/m^3$, corresponding to an n = .59 and $K \cong 3$. For a visual range of 10 KM, $n \cong 1.26$, $r/\lambda \approx .65$, $\langle r \rangle = .33\mu$, $K \cong 3$ and $\langle N \rangle \cong 3.8 \times 10^8/m^3$. Consequently, we are to assess the effects of water droplets in the range of $4 \times 10^8/m^3$ to $2 \times 10^9/m^3$, varying in size from .4 to $.3\mu$ for the infrared and the microwave regions.

Before addressing this problem, it is instructive to compare the obscuring power of rainfall with that of haze considered above. It can be shown that[11],

$$\sigma = 5.2 \times 10^{-6} X (cm^{-1}) \qquad (14)$$

where X = number of raindrops/cm^2-sec and the drops are large enough for K to be 2 (greater than 10λ). From equation (7) and noting that Z, the precipitation rate (cm/sec.), is Xv_r where v_r is the volume of a single raindrop, we have that,

$$Z\,(cm/sec) \cong \frac{.75 \times 10^6 \, v_r (cm^3)}{V_2 (cm)} \qquad (15)$$

Assuming a raindrop size of 1 mm radius, we have that,

$$Z\,(cm/sec) \cong \frac{\pi \times 10^5}{V_2\,(cm)} \tag{16}$$

Consequently, for a V_2 of 1 KM (10^5cm), $Z = \pi \times 10^{-2}$ and for V_2 = 10 KM, $Z = \pi \times 10^{-3}$ cm/sec. As rainfall seldom exceeds 2 to 3"/hr., we conclude that rainfall can have less obscuring power than haze (i.e. greater visual range). These results will be used when considering the infrared and microwave regions.

In order to assess the effect of haze in the infrared and microwave regions, we utilize the general form of the extinction coefficient from the Mie theory. For an absorbing particle with a complex refractive index (water in the infrared and microwave), the scattering coefficient for values of $\alpha < 1$ is given by,

$$Q_s = \frac{2\lambda^2}{3\pi}\,\alpha^6\,|k|^2 \tag{17}$$

where $k = (m^2 - 1)/(m^2 + 2)$. The absorbtion coefficient is given by,

$$Q_a = \frac{\lambda^2}{\pi}\,\alpha^3\,Im\,(-k) \tag{18}$$

where Im is the imaginary part of $-(m^2 - 1)/(m^2 + 2)$. Equations (17) and (18) combined produce the extinction coefficient per particle and can be related to σ of the visual range by multiplying by $\langle N \rangle$ calculated above.

For water droplets in the infrared, the complex refreactive index at 6μ is,

$$m^* \cong 1.304 - .1\,i \tag{19}$$

For water spheres with $\langle r \rangle \cong .35\mu$, $\alpha \cong .37$. From equation (19), $(m^*)^2 = 1.69 - .26i$ and $k = .18 - .08i$ with $k^2 = .04$. Accordingly, $Q_s = 7.8 \times 10^{-16}$ m^2 and $Q_a = 4.64 \times 10^{-14}$ m^2. Consequently, $Q_t = 4.7 \times 10^{-14}$m^2. From the visual range, the maximum $\langle N \rangle$ was found to be about $2 \times 10^9/m^3$. Hence $\sigma = 9.4 \times 10^{-5}\,m^{-1}$ or $\sigma = .094$ KM^{-1}. In

terms of optical depth used in section III, part A, even at 2 KM, the effect on the τ due to water droplets is not significant compared to the τ of water vapor. Consequently, we conclude that even with a visual range of 1 KM, the effect on the infrared measurement is not significant. In the case of rainfall, the effect would be about the same as in the visible as $\alpha > 10$ and the extinction coefficient is nearly the same for absorbing and non-absorbing particle.

For the microwave region for haze particles, as the value of α is so small ($\sim 10^{-4}$), only Rayleigh scattering prevails and the effect on σ of the oxygen band ($\sim$5mm) is even less than the infrared region. However, for rainfall, where the drop size is comparable to the microwave wavelength, equations (18) and (19) can be used. The values for $|k|^2$ and Im (-k) for water at .62cm has been tabulated[14] and the attentuation coefficient per mm rainfall/hr. has been calculated by Medhurst[15]. At 60 GHz (oxygen frequency), the maximum rainfall attenuation coefficient measured is about .85 DB/KM per mm/hr. From the previous calculation utilizing the visual range it was estimated that a visual range of 10 KM corresponds to a rainfall of about 10 cm/hr. (a rate only occuring for a short time at frontal regions). If we assume a rainfall of 1 cm/hr. (corresponding to a heavy downfall), then it is expected that there will be an appreciable effect on the microwave method as the ground value for oxygen absorbtion is about 14 DB/KM.

It is concluded from the above analysis that for visual ranges of 1 to 10 KM due to haze or fog, the infrared and microwave methods are not significantly affected and will not result in appreciable errors; however, for rainfall, the microwave region is affected more than the infrared and corrections are necessary to utilize the method.

VI. RECOVERY OF TEMPERATURE AND WATER-VAPOR PROFILES FROM THE PASSIVE PROBES

Rather than examining every combination of temperature and water-vapor distributions, which would detract from the main goals of this study, we examine in this section, a temperature distribution with two inversions combined with a water-vapor distribution with five inversions up to two kilometers. The rationale for this combination stems from the belief that this combination represents a worse case and if these distributions can be recovered satisfactorily, then any combination having less inversions will also be recovered satisfactorily.

The temperature profile used is depicted in figure 5 and the water-vapor profile used in combination is shown in figure 6. Although this may not represent a real case, the results should be an indication of the enormous potential of the passive method.

A. Temperature Profile Analysis

As mentioned in the previous sections, the measured temperature by a microwave radiometer at the ground due to a given distribution is given by,

$$T_M = T_o\left(1-e^{-\Phi_o \Delta h}\right) + T_1 e^{-\Phi_o \Delta h}\left(1-e^{-\Phi_o \Delta h}\right) + \cdots \qquad (1)$$

where, T_o is the ground temperature, Δh is the increment of height, Φ_o is $k_o \sec \theta$, k_o is the ground value oxygen attenuation coefficient, θ is the zenith angle and T_n is the temperature of each succeeding layer. If we let $x = e^{-\Phi_o \Delta h}$, then we have that,

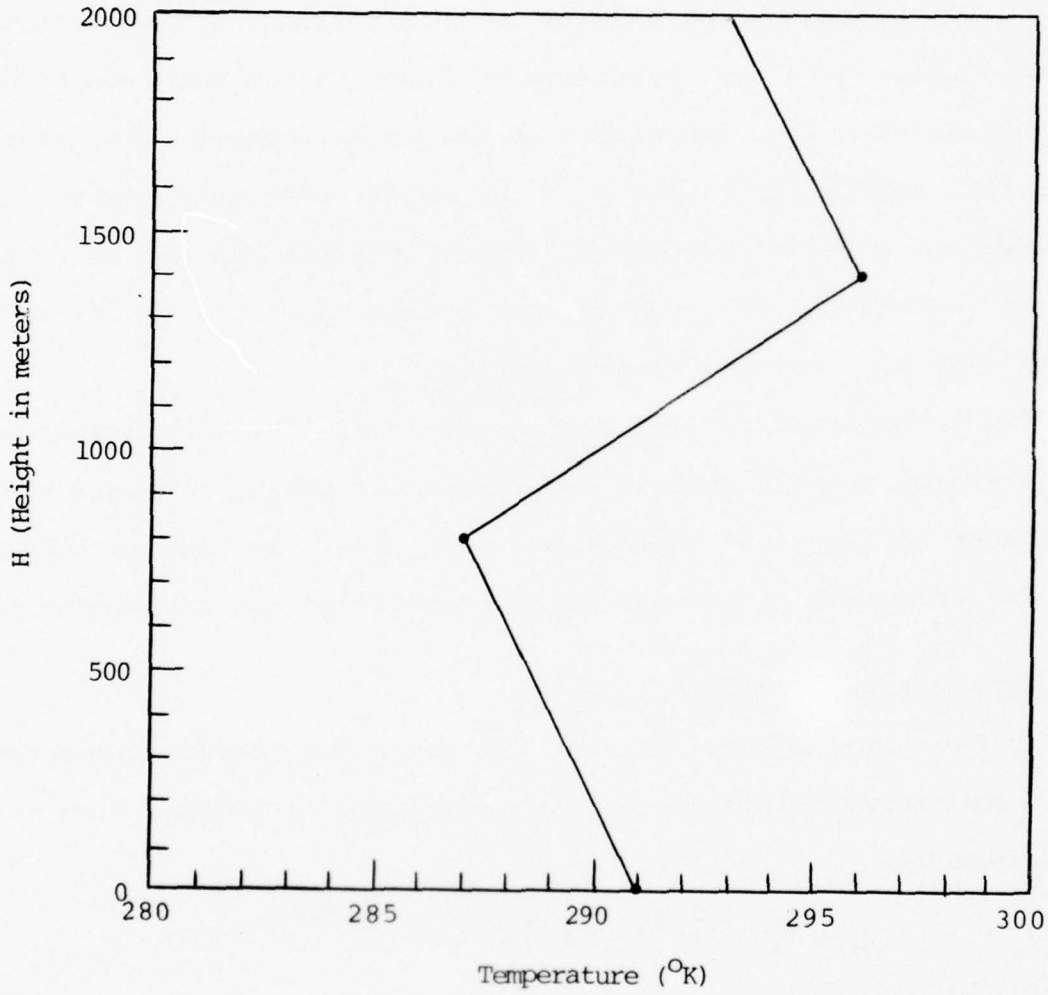

FIGURE 5. TEMPERATURE PROFILE USED IN CALCULATIONS IN TEXT

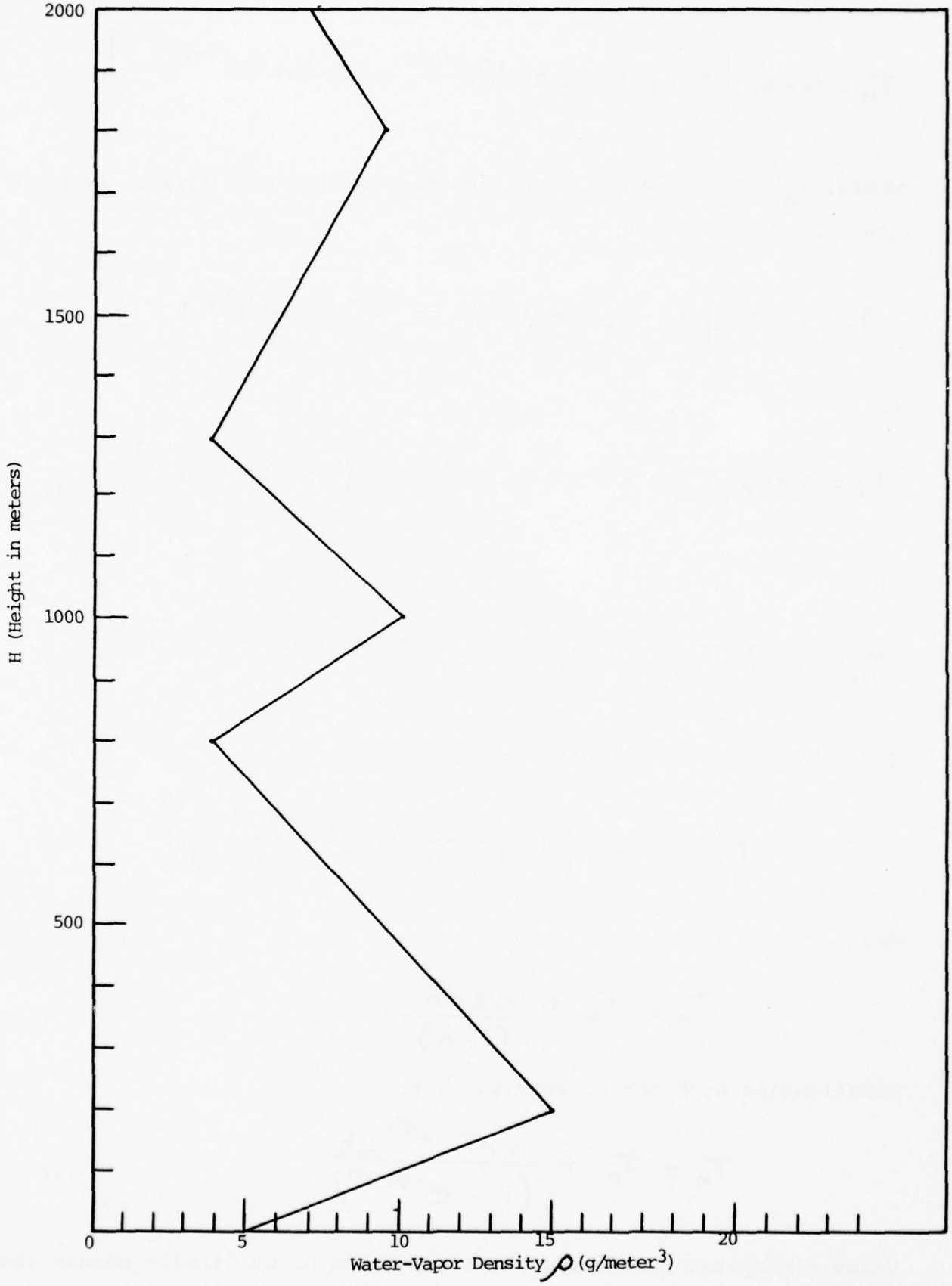

FIGURE 6. WATER-VAPOR DENSITY PROFILE USED IN CALCULATIONS IN TEXT

$$T_M = (1-x)\left[T_o + (T_o + a\Delta h)e^{-\phi_o \Delta h} + (T_o + 2a\Delta h)e^{-2\phi_o \Delta h} + \cdots\right] \quad (2)$$

where, $T_n = T_o + na\Delta h$ (linear gradient within each layer). Rearranging (2) we have that,

$$T_M = (1-x)\left[T_o + (T_o + a\Delta h)x + (T_o + 2a\Delta h)x^2 + \cdots\right] \quad (3)$$

or,

$$T_M = (1-x)\left[T_o\{1 + x + x^2 + x^3 + \cdots\} + a\Delta h\{x + 2x^2 + 3x^3 + \cdots\}\right] \quad (4)$$

or,

$$T_M = (1-x)\left[T_o\{1 + x + x^2 + \cdots x^N\} + ax\Delta h\{1 + 2x + 3x^2 + \cdots Nx^{N-1}\}\right] \quad (5)$$

If we let N go to infinity, we have that,

$$T_M = (1-x)\left\{T_o\left(\frac{1}{1-x}\right) + ax\Delta h\left(\frac{1}{(1-x)^2}\right)\right\} \quad (6)$$

or,

$$T_M = T_o + \frac{ax\Delta h}{(1-x)} \quad (7)$$

Substituting back for x, we have that,

$$T_M = T_o + \frac{a e^{-\phi_o \Delta h}\,\Delta h}{(1 - e^{-\phi_o \Delta h})} \quad (8)$$

Using L'Hospital's rule and letting Δh go to 0, we finally obtain that,

$$T_M = T_o + \frac{a}{\Phi_o} \qquad (9)$$

This represents the integrated value of measured temperature. It is interesting to note , that this same result was obtained in section III, equation (11) using an entirely different approach.

If the Δh remains finite, then the equivalent to equation (9) is given by,

$$T_M = T_o + a\Delta h \times \left\{ \frac{1 - X^N}{1 - X} - N X^N \right\} \qquad (10)$$

where N represents the number of layers taken with a given Δh.

We have programmed both equations (9) and (10) for the temperature profile given in figure 1. We have compared the T_M for $\Delta h = o$ (true measured temperature) with $\Delta h = 50, 100$ and 200 meters. The results of these computations are not reproduced in this report.

The integrated case results (i.e. what is measured by the radiometer) is shown in figure 7 for the temperature profile of figure 5. The actual values of Φ_o used for the computation were:

(1) .030/meter

(2) .021/meter

(3) .010/meter

(4) .005/meter

(5) .003/meter

(6) .001/meter

For the .001/meter case, it was necessary to integrate up to 6.4 km. using a constant gradient, 2 km on. This point was excluded from figure 7. For the .003 case, the integration went to 3.6 km before reaching a

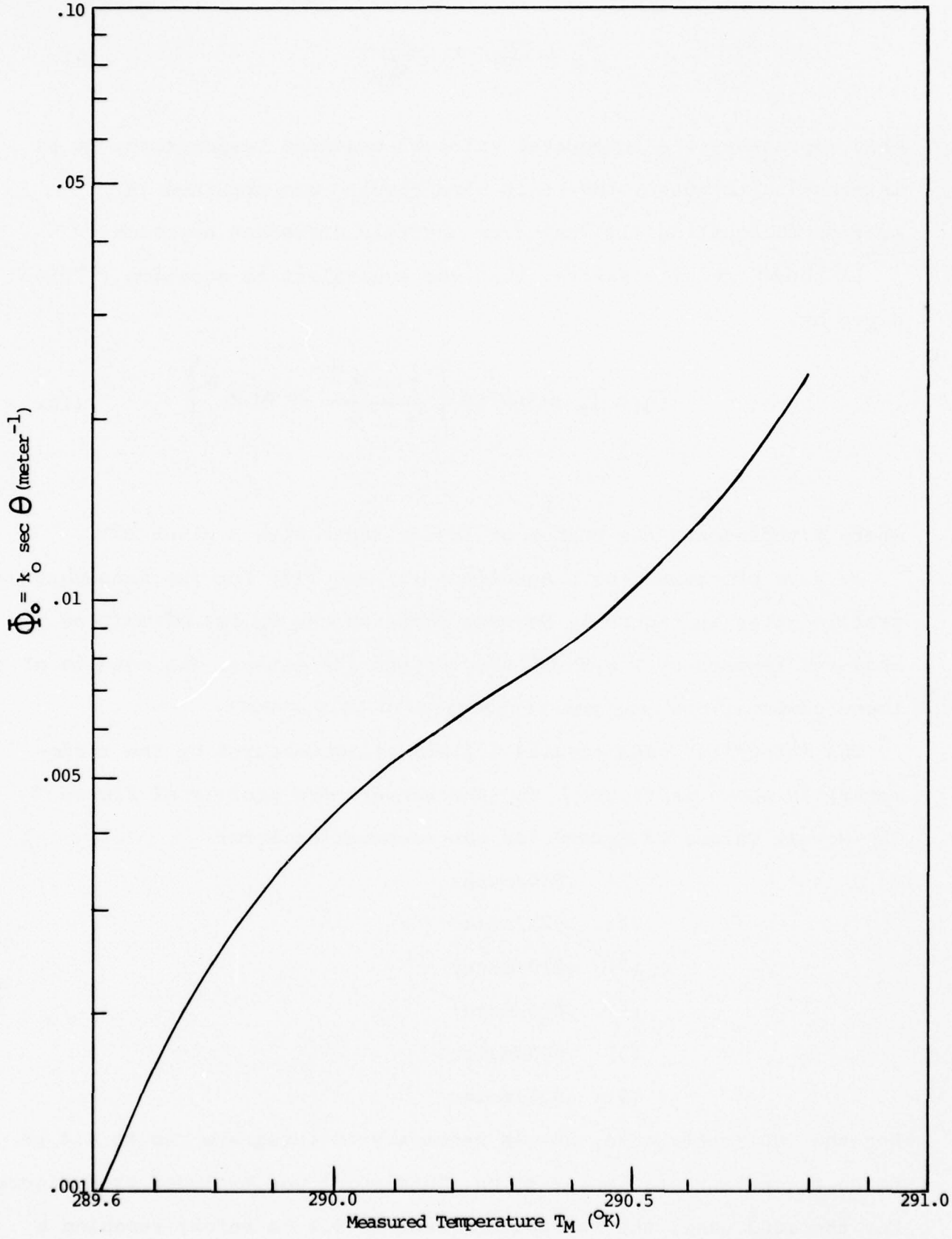

FIGURE 7. CALCULATED MEASURED TEMPERATURE AS A FUNCTION OF Φ_o

constant value. For the .005 case, it stabilized at about 2 km with the other cases stabilizing at less than 2 km.

From the results of these computer calculations, we were able to determine the cut-off height over which a given Φ_o is effective. This is shown in figure 8. It is to be noted that for values of Φ_o less than .0025, the cut-off height is greater than 2 km. Consequently, in practice, we would utlize values of Φ_o equal to.002 or greater.

According to equation (9), a measurement of T_M at given Φ_o will result in an apparent a. We have calculated the apparent a as a function Φ_o. This is shown in figure 9. As noted from the figure, the apparent a remains constant until about $\Phi_o = .007$. From figure 8 the effective cut-off is 700 meters. Consequently, we can conclude that above 700 meters there is a change in gradient.

In order to recover the profile of figure 5, we would conclude that up to 700 meters, the gradient is constant and changes above 700 meters. The gradient for the first 700 meters is computed from equation (9). Consequently, any temperature measurement from Φ_o equal to .021 to .007 would yield a gradient of $-.005^{o}K$/meter. In order to recover the rest of the profile we note that, for a temperature distribution with inversions we have that,

$$T_M = T_o + a_1/\Phi_o + a_2/\Phi_o e^{-\Phi_o H_1} + a_3/\Phi_o e^{-\Phi_o H_2} + \ldots \quad (11)$$

Since the apparent gradient is given by,

$$T_M = T_o + a/\Phi_o \quad (12)$$

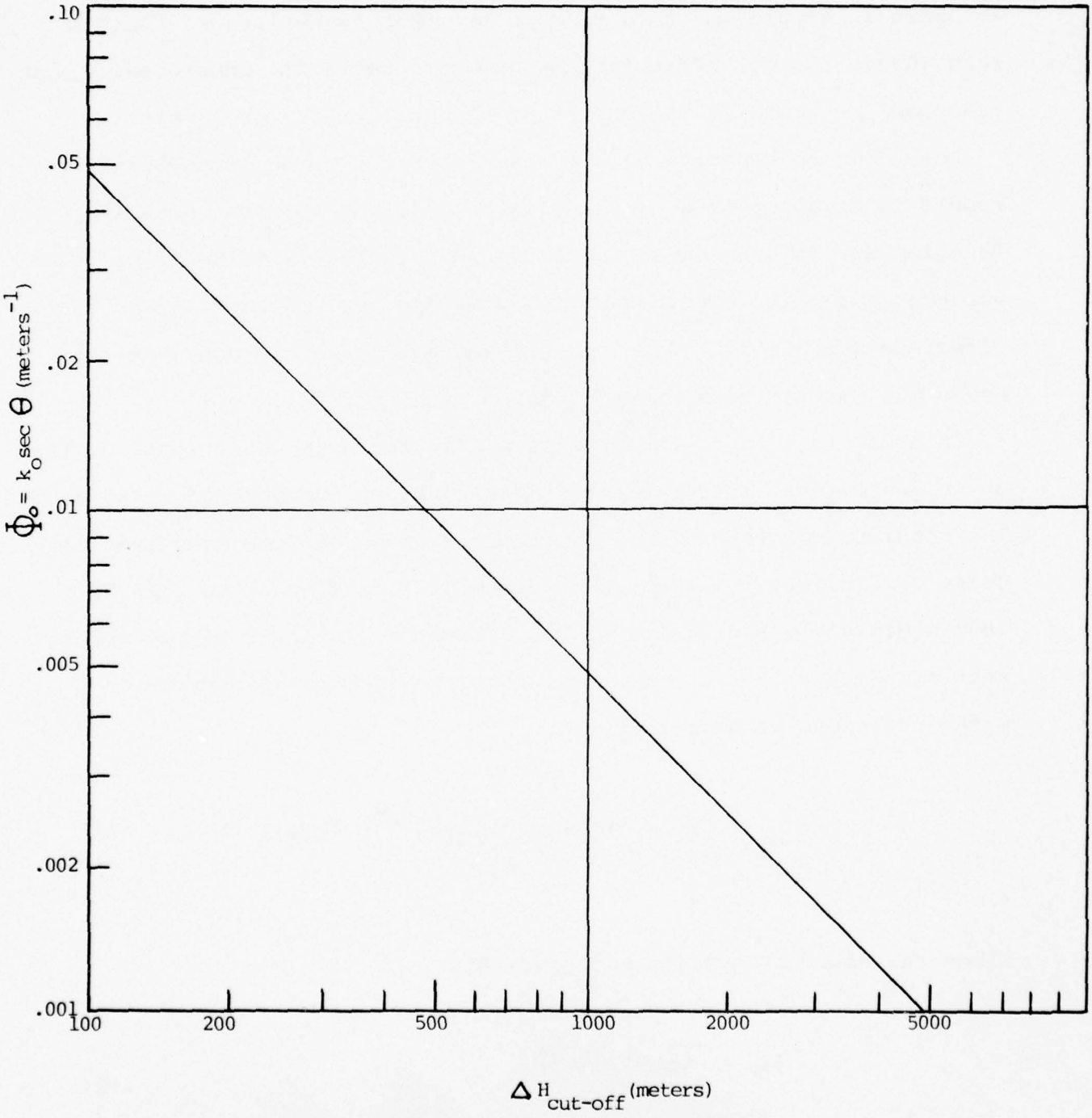

FIGURE 8. EMPIRICALLY DETERMINED $\Delta H_{CUT\text{-}OFF}$ VERSUS Φ_o (SEE TEXT)

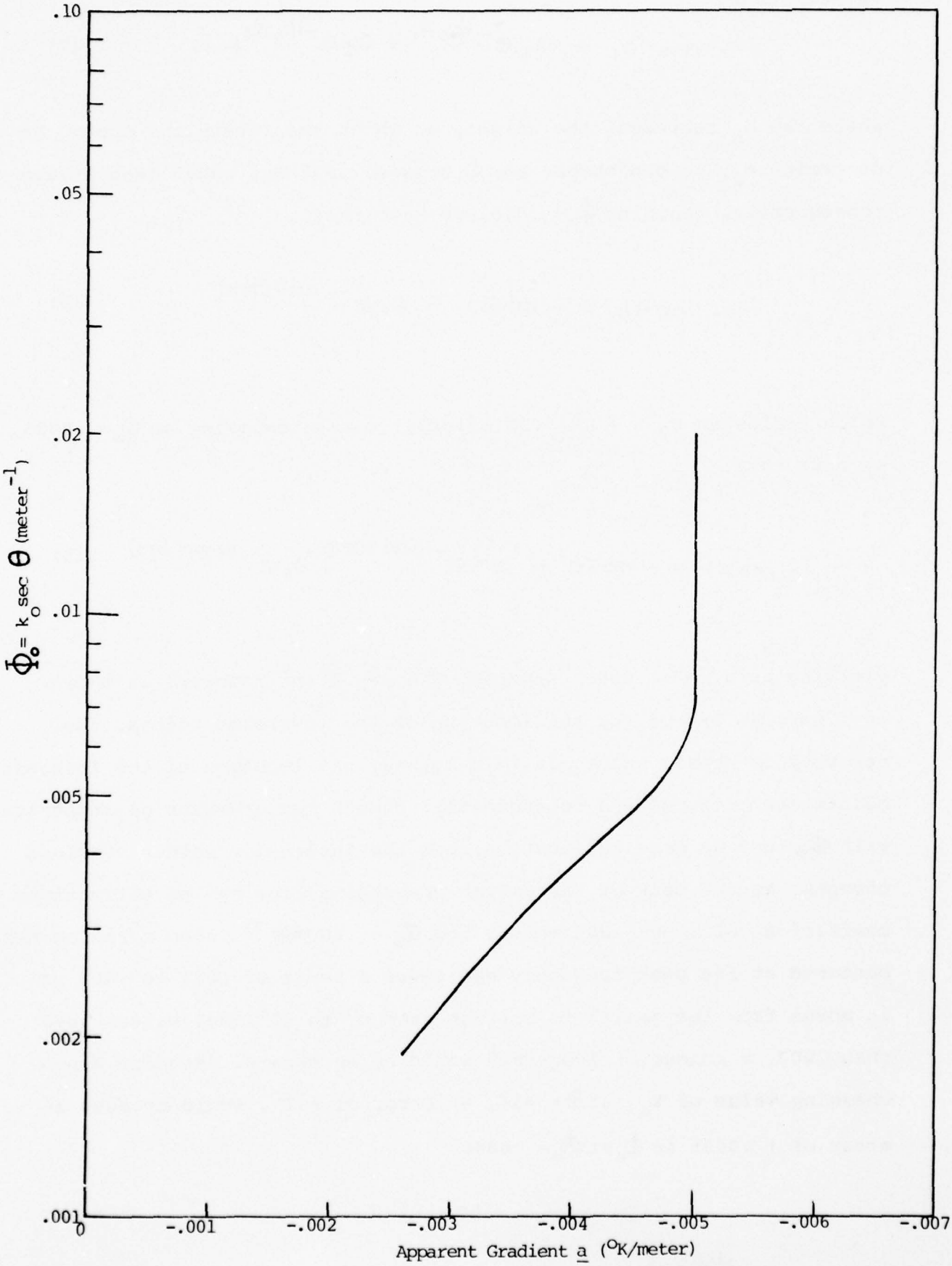

FIGURE 9. APPARENT GRADIENT CALCULATED FROM MEASURED TEMPERATURE

we have that,

$$a = a_1 + a_2 e^{-\phi_o H_1} + a_3 e^{-\phi_o H_2} + \ldots \qquad (13)$$

where the H_n represent the heights at which the inversions occur. To determine a_2, we can choose any ϕ_o between .007 and .0035 (see figure 9). Consequently, choosing $\phi_o = .005$, we have that,

$$-.0046 = -.0050 + a_2 e^{-.005(700)} \qquad (14)$$

which yields an $a_2 = +.013$. Similarly, for a_3 choosing an $\phi_o = .0025$, we have that,

$$-.0031 = -.0050 + .013 e^{-.0025(700)} + a_3 e^{-.0025(1375)} \qquad (15)$$

yielding an $a_3 = -.0093$ ^{o}K/meter. The resultant recovery is shown in figure 10. Except for the location of the inversion points, the recovery is nearly exact. In this method, the location of the inversion points are critical and consequently, enough measurements of temperature with ϕ_o must be made to locate either the inflection points or slope changes. As the peak of the oxygen absorption line has an extinction coefficient of about .003/meter, and $\phi_o = .003 \sec \theta$, then a radiometer centered at the peak frequency can cover a range of .021 to .003 as it moves from the zenith to horizon from 0^{o} to 82^{o}. For values less than .003, a change of frequency would be necessary. Assuming a non-changing value of k_o, at $\theta = 45^{o}$, an error of $\pm 1^{o}$, would produce an error of $\pm$ .0001 in ϕ_o at $\phi_o = .0040$.

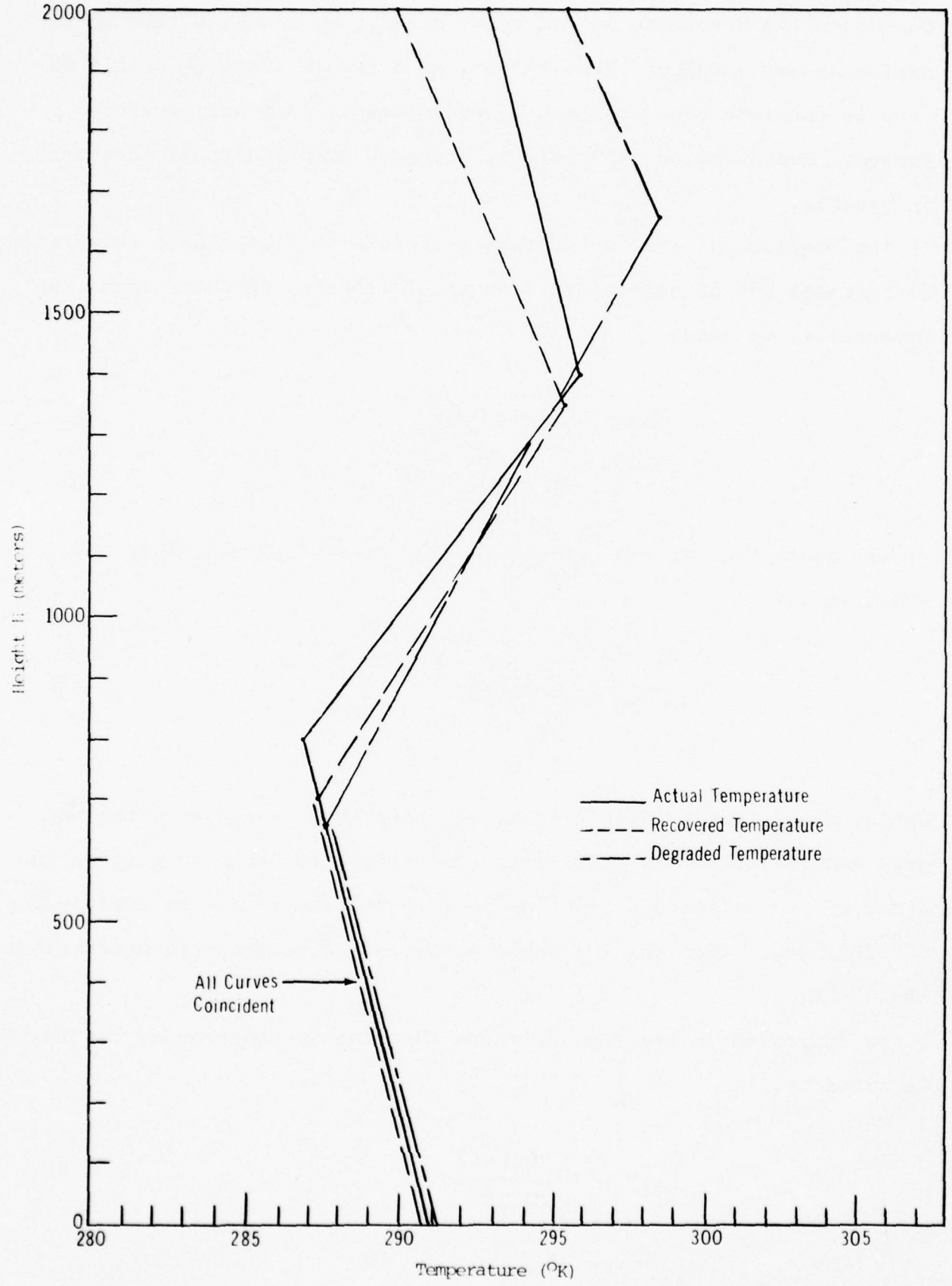

FIGURE 10. RECOVERED AND DEGRADED TEMPERATURE PROFILES
(SEE TEXT)

Consequently, depending on the value of Φ_o, we conclude that we can differentiate a $\Delta\Phi_o$ of .0005 easily. As a result, from Φ_o = .010 to .003 we conclude that at least 15 measurements in θ are possible. However, depending on the profile, 15 measurements are not necessary in general.

The requirement that a radiometer be able to distinquish temperature differences can be determined from the following. In determining the apparent a, we used,

$$T_M = T_o + a/\Phi_o \tag{16}$$

If we assume that T_o can be measured accurately and that Φ_o is not limiting then,

$$\Delta T_M = \Delta a/\Phi_o \tag{17}$$

Consequently, the tolerable error in temperature depends on the Φ_o used and the tolerable error on a. The tolerable error on $\underline{a}$ is on the order of 5%. Assuming an average $\underline{a}$ of .005 ^oK/meter and an average Φ_o of .005/meter, then the tolerable error on the temperature measurement is .05 ^oK.

As expressed in section IV, there the minimum temperature resolvable is given by,

$$T_{MIN} = \frac{C(N-1)}{\sqrt{Bt}} \tag{18}$$

where, the symbols have the previous meanings. To achieve a system

temperature noise of .05°K would require an integration time of 10 sec. with a bandwidth of 60 MHz and a system noise of 4 DB. Although this would be a sophisticated system, it is within the state-of-the-art.

In order to determine the extent of the degradation of the profile recovery, we will assume an error on the slope measurement of ± 5%. In addition, we will assume that the error on Φ_o is not limiting and proceed to determine the recovery possible. It must be noted that this is a gradient method as opposed to a spatial method (e.g. Lidar back-scattering). If there are no inversions, then the error on the gradient is just ± 5% as only one measurement is necessary. For example, for a typical gradient of - .005 °K/meter, the error at 2km for a base temperature of 291.00 °K is just ± 0.5 °K. If there is one inversion, then the location of the inversion position is critical and the error is greater. For the profile under consideration, we impose an error of ± 5% and proceed to determine the extent of the deterioration. At an $\underline{a}$ of - .005 °K/meter, a change in $\underline{a}$ of ± .0003 is necessary to distinguish a real difference in slope. The first inversion point (change in slope of figure 9) could occur anywhere between a Φ_o of .0075 to .005 which from figure 8 corresponds to an H of 650 and 950 meters respectively.

As a_2 is derived from,

$$a(\text{due to } a_2) = a_2 e^{-\Phi_o H_1} \tag{19}$$

then,

$$\Delta a = -\Phi_o a_2 e^{-\Phi_o H_1} \Delta H \tag{20}$$

For a $\phi_o = .005$ and an $a_2 = +.015$ (actual value) the error in $\underline{a}$ due to an error in the placement of the inversion height becomes,

$$\Delta a = 7.5 \times 10^{-5} e^{-.005(800)}(150) \tag{21}$$

where we have used an error of $\pm$ 150 meters on H. Then the error in the apparent gradient is,

$$\Delta a = \pm 2.0 \times 10^{-4} \tag{22}$$

This error is consistent with our previous remarks on the distinguisbability in $\underline{a}$. Similarly, the error in the apparent $\underline{a}$ due to a_3 is,

$$\Delta a = \pm 2.5 \times 10^{-3}(5 \times 10^{-3}) e^{-.0025(1400)}(150) \tag{23}$$

or,

$$\Delta a = \pm 5.7 \times 10^{-5} \tag{24}$$

The combined error for a two inversion system is just

$$\Delta a = \pm \sqrt{(\Delta a_2)^2 + (\Delta a_3)^2} \tag{25}$$

or,

$$\Delta a = \pm 2.1 \times 10^{-4} \tag{26}$$

Consequently , we conclude that for an error in placement of the inversion heights of ± 150 meters in a two inversion system, the error in a is on the order of ± .0002.

From the analysis above we can now construct a degraded profile. We place the inversion heights at the extremes (i.e. first inversion at 650 meters and the second inversion at 1650). For the first gradient we have that,

$$a = a_1 + a_2 e^{-\phi_0 H_1} \tag{27}$$

then,

or,

$$a_2 = (+.0004 \pm .0003) e^{.005(650)} \tag{28}$$

$$\boxed{a_2 = +.010 \pm .008} \tag{29}$$

For a_3, with H_2 at 1650, we have that,

$$-.0031 \pm .0002 = -.005 \pm .00025 + [.010 \pm .008] e^{-.0025(650)} + a_3 e^{-.0025(1650)} \tag{30}$$

or,

$$+.0019 \pm .0003 = +.0020 \pm .0016 + a_3(.0162) \tag{31}$$

or,

$$\left(-.0001 \pm .0016\right)\left(1.62 \times 10^{-2}\right) = \boxed{a_3 = -.0062 \pm .010} \qquad (32)$$

Using these values we constructed the degraded profile which is shown in figure 10, labeled degraded profile, using the average values derived above.

Again we conclude that the recovery of the temperature profile is satisfactory. Except for the exact placement of the inversion heights, the recovered profile is adequate for the intended use in radio-wave propagation.

B. Water-Vapor Profile Analysis

Although originally we had proposed to recover the water-vapor profile spatially, we now believe that the application of the gradient method used for the temperature recovery is a more powerful technique requiring less measurements and leading to better recovery.

The equivalent water-vapor density integrated along the line of sight is given by,

$$W = \int_{h_1}^{h_2} P/P_o \left(\frac{T_o}{T}\right)^{1/2} \rho \, dh \qquad (1)$$

where the symbols have the previous meanings. If we assume that P_o and T_o are the conditions at h_1 and P and T the conditions at h_2 then,

$$W \cong \frac{P}{P_o}\left(\frac{T_o}{T}\right)^{1/2} \int_{h_1}^{h_2} \rho \, dh \qquad (2)$$

In addition if we linearize the density profile between h_1 and h_2 we

$$\rho = \rho_o + ah \tag{3}$$

where $\underline{a}$ is the gradient between h_1 and h_2. Substituting we have that,

$$W \cong \frac{P}{P_o}\left(\frac{T_o}{T}\right)^{1/2}\left[\int_{h_1}^{h_2}\rho_o dh + a\int_{h_1}^{h_2} h\,dh\right] \tag{4}$$

Integrating we have that,

$$\frac{a}{2} \cong \frac{W\frac{P_1}{P_2}\left(\frac{T_2}{T_1}\right)^{1/2} - \rho_o(h_2-h_1)}{(h_2^2 - h_1^2)} \tag{5}$$

If we let $h_1 = 0$ (i.e. at the ground) then,

$$\frac{a}{2} \cong \frac{W\frac{P_o}{P}\left(\frac{T}{T_o}\right)^{1/2} - \rho_o h}{h^2} \tag{6}$$

Consequently, with ground conditions known, (i.e. ρ_o, P_o, T_o and the temperature profile known) a measurement of W allows the determination of the gradient. In addition, as the expression is not very sensitive to the temperature ratio we can write,

$$\frac{a}{2} \cong \frac{W\,P_o/P - \rho_o h}{h^2} \tag{7}$$

The ratio P_o/P we have utilized is the standard pressure gradient as deviations are not great.

In order to utilize equation (7), we have choosen increments of 200 meters to extract 10 measurements to probe up to 2 km. Larger increments could be used; however, due to the fact that the water-vapor profile tends to have a greater number of inversions then the

Assuming a temperature profile is known, (previous example) we first calculate the saturated water-vapor profile W, consistent with the temperature profile. This is shown in figure 11. This was computed exactly from equation (1). Shown also in figure 11 is the calculated W for the water-vapor distribution given in figure 6.

From section IV, part B, figure 3, we can calculate the Φ necessary for the saturated case to produce a W of .3 gms/cm^2 at 200 meters. From figure 3, Φ = 9.50. For the actual profile, at 200 meters, Φ = 11.80 for W = .20 gm/cm^2. At this Φ, the radiometer would produce an SNR consistent with a change of W= .20 (figure 3, section IV, part B, top curve).

Proceeding in this fashion we go to the next 200 meters and so on. Table I shows the result of this procedure.

TABLE I

H (meters)	W (pr. cms.)	Φ
2000	1.43	3.95
1800	1.30	4.15
1600	1.16	4.40
1400	1.06	4.65
1200	.98	4.90
1000	.84	5.30
800	.72	5.75
600	.62	6.20
400	.45	7.50
200	.20	11.80

With these values of W, we can reconstruct the profile. For the first 200 meters, applying equation (7) we obtain an $\underline{a}$ = + .050 g/m^3/ meter. Since ρ_o is 5 g/m^3, then at 200 meters it is 15 g/m^3. Continuing in this fashion we obtain Table II. The resulant profile is shown in figure 12. As can be seen, the recovery is remarkable. The only major

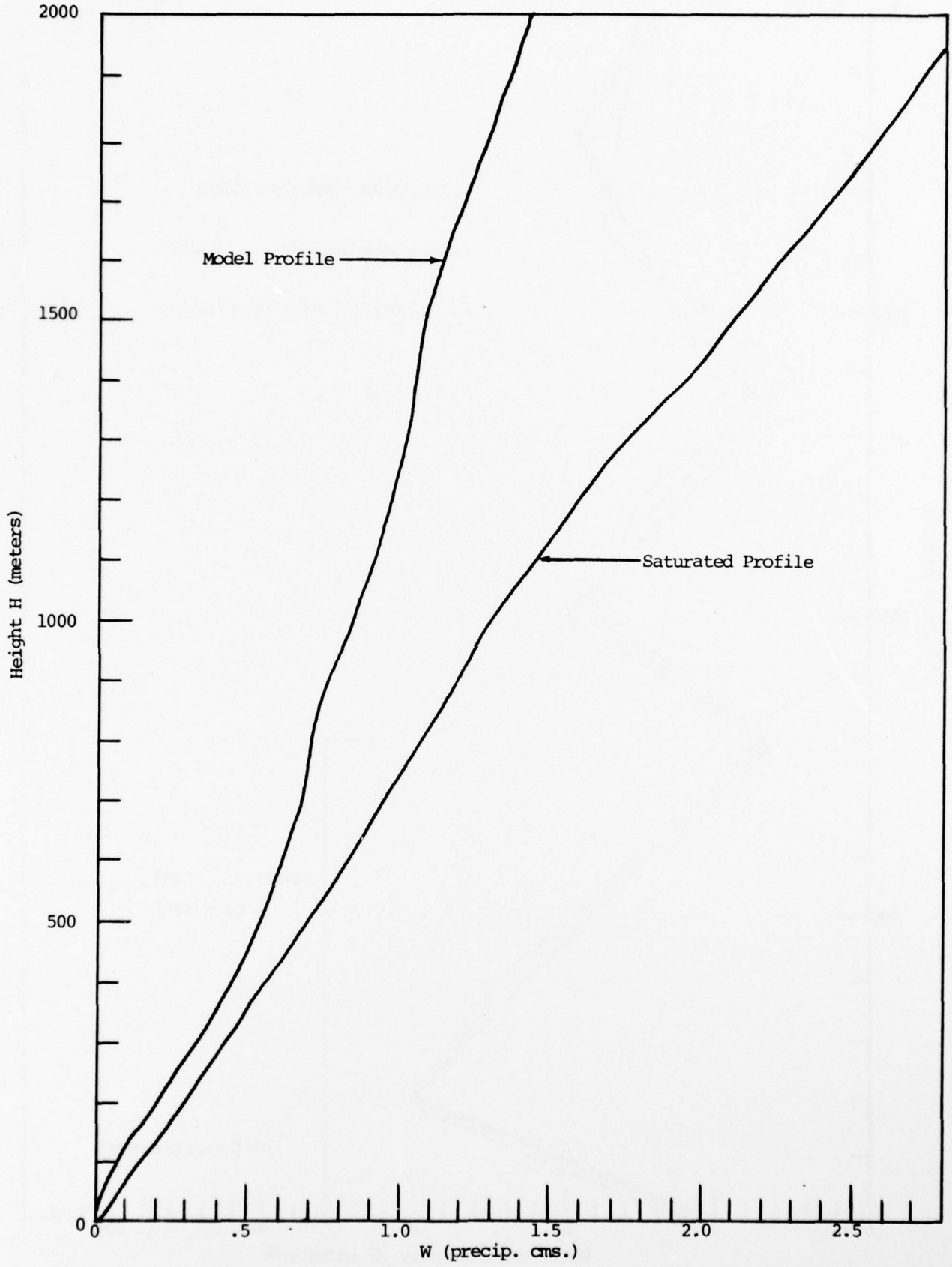

FIGURE 11. CALCULATED W FOR SATURATED AND MODEL PROFILES (SEE TEXT)

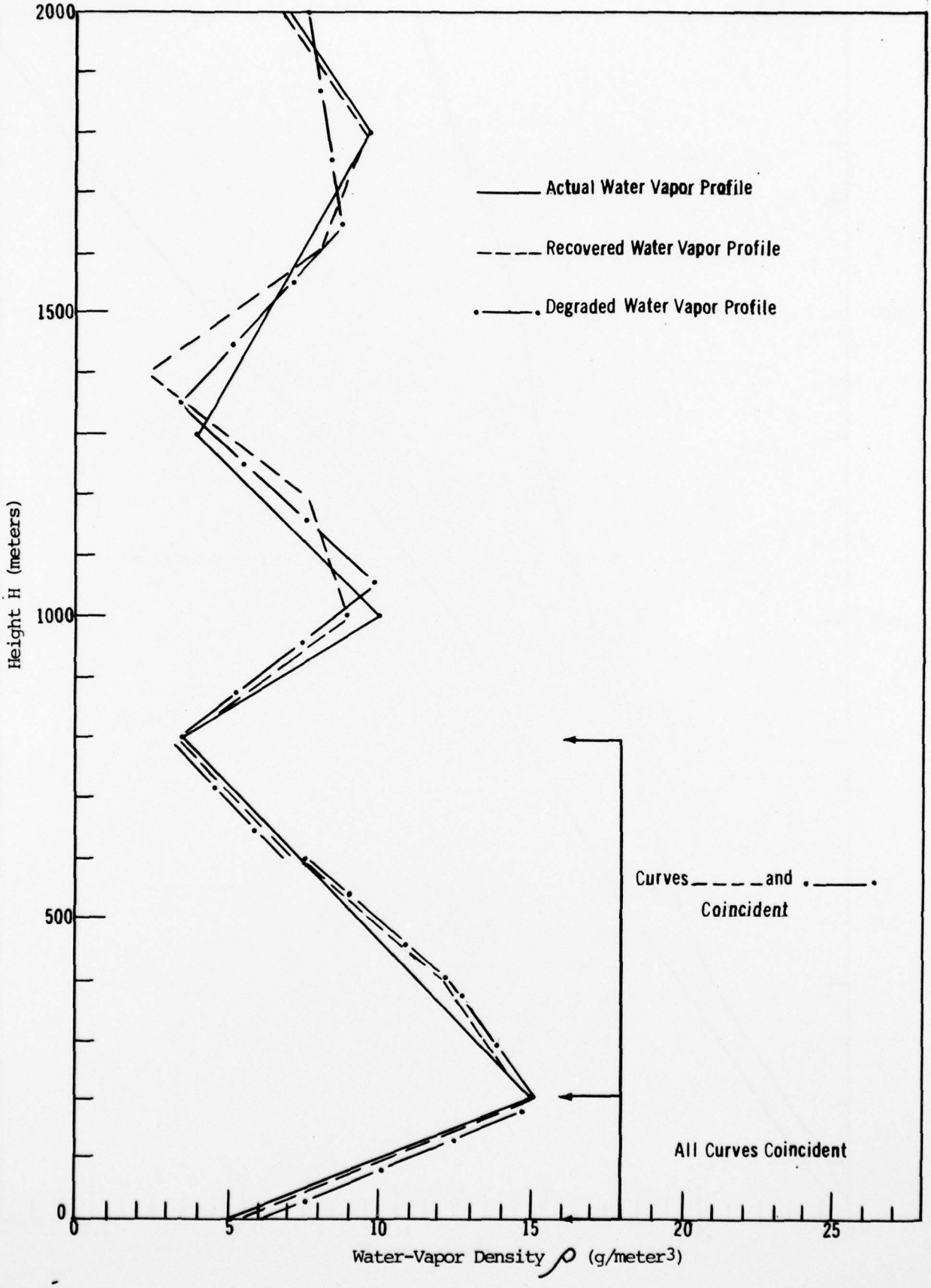

FIGURE 12. RECOVERED AND DEGRADED WATER-VAPOR DENSITY PROFILES

error occurs when an inversion falls between a 200 meter increment; however, the procedure tends to average and recovers the profile well above the inversion point (see top of the recovery curve).

TABLE II

H (meters)	W (pr. cms.)	P_1/P_2	a
0 to 200	.20	1.03	+.050
200 to 400	.45	1.05	-.019
400 to 600	.62	1.08	-.028
600 to 800	.72	1.11	-.009
800 to 1000	.84	1.13	+.022
1000 to 1200	.98	1.17	-.008
1200 to 1400	1.06	1.19	-.026
1400 to 1600	1.16	1.22	+.039
1600 to 1800	1.30	1.25	+.008
1800 to 2000	1.43	1.28	-.012

In order to evaluate the expected error,we note that in Table I, we have tacitly assumed that differences on the order of $\Delta\Phi = 0.1$ can be measured. However, we showed in section IV, TableI, that the measurable difference in Φ is dependent on the actual profile. For this case we proceed as follows. The measured W at the first 200 meters is 0.20 g/m^2. The next measurable W at an SNR = 1 can be determined by consideration of the following. At 400 meters, W_2 = .45 and Φ = 7.50. Hence $-\delta = 0.23$. From figure 3, section IV, part B , at Φ = 7.50 and an $-\delta = 0.23$, the SNR is well above 1 and can be measured. At 600 meters, W_2 = .62 and Φ = 6.20 with $-\delta = 0.12$, the SNR is still above 1. At 800 meters, W_2 = .72 at Φ = 5.75 with $-\delta = .07$ which is just measurable. Consequently, above 800 meters, the recovered profile will begin to degrade. The next measurable W occurs at about 1050 with a W_2 = .88 and Φ = 5.20. This requires a recalculation of a . Continuing in this manner results in the degraded profile shown in figure 12 labeled degraded. As can be seen, except for the locations

of the inversion heights, the degraded profile follows the true profile remarkably well.

It is to be noted in passing that the gradient technique works well, as it appears that it can tolerate greater errors without degrading the true profile appreciably more so than a spatial technique.

VII CONCLUSIONS AND RECOMMENDATIONS

The primary motivation for this study was to determine the feasibility of using the existing technology of infrared and microwave radiometers to measure the verical distributions of atmospheric temperature and water-vapor. This information was necessary to correct for radio wave refractive index in order to adequately predict the radio wave trajectory.

This study has shown that:

1) high spatial resolutions of temperature and water-vapor distributions are not necessary for predicting the radio wave trajectory

2) for angles of elevation greater than 30^{o} off the horizon with a tolerable error on angle trajectory of $.1^{o}$ or greater, a standard atmospheric gradient model is sufficient for radio wave propagation

3) unless intial trajectories of the radio wave are close to the horizon (less than 1^{o}), the vertical distribution of temperature and water-vapor obtainable from the passive probes are more than adequate for radio wave propagation corrections

4) temperature profiles are obtainable using the natural microwave radiation from atmospheric oxygen from a gradient technique

5) water-vapor profiles are obtainable using the natural radiation in the infrared from atmospheric water-vapor from a gradient technique

6) spatial resolutions obtainable by both methods are more than adequate to describe radio wave propagation for most applications

7) both methods are capable of probing for temperature and water-vapor up to 2 kilometers

8) low visibility does not interfer with either probe appreciably

9) suuficient number of measurements (i.e. distinct) can be made to accurately track at least 5 inversions in water-vapor and at least 2 inversions in temperature

10) no new technology is necessary to implement the fabrication of a temperature/water-vapor probe

Although the mathematical excursions used in the previous sections to determine feasibility have been rather unwieldy, the actual implementation of the technique is remarkably straight foward. The necessary computations and comparsions that must be made in real time can easily be accomplished by a dedicated microprocessor/controller. This system must be interfaced with the radiometer along with local sensors for temperature, pressure and humidity. If properly implemented, the gradient technique appears to be less sensitive to experimental errors than a spatial technique either active or passive and holds the potential of becoming a more reponsive probe than either Lidar or passive probes using weigthing functions.

It is recommended that the next phase of study should be a design phase in which the integration of a microprocessor/ controller with local sensors and existing radiometer be examined. As a first step, it is recommended that this design study begin with an existing

infrared radiometer to be modified for integration of sensors and computer. The infrared radiometer should be examined first as it is believed that the microwave radiometer system may require more of an effort. Consequently, we recommend the following task items in a future study:

1. Begin design study for integration of pressure,temperature and humidity sensors with a microprocessor/contoller.
2. Work with an established infrared firm (e.g. Barnes Engineering) to custom design or modify and existing infrared radiometer.
3. Begin design of microcomputer (in liaison with an existing computer firm such as Mostek) to establish dedicated ROM's for the necessary on-line calulations along with RAM's for processinf the in-coming data.
4. Integrate efforts with infrared and computer companies to develop a system suitable for carrying out the determination in real time the water-vapor density profile.

REFERENCES

(1) Erich W. Marchand, J.O.S.A., 60, I, pg. 1, Jan. 1960.

(2) C.W. Allen, "Astrophysical Quantities", the Athlone Press, University of London, pg. 105, 1955.

(3) V.J. Falcone, Jr. and R. Dyer, AFCRL-70-0007 Jan. 1970, No. 214.

(4) R.M. Goody, "Atmospheric Radiation", Oxford, Clarendon Press, 1964.

(5) E.R. Westwater, Radio Science, Journal of Research NBS/ USNC-URSI, 69D, No. 9, Sept. 1965, pg. 1201.

(6) M.L. Meeks and A.E. Lilley, J. GEO. Res., 68, No. 6, Mar. 1963, pg. 1683.

(7) E.R. Westwater and R.L. Abbott, NBS report 8799, U.S. Dept. of Commerce, March 1965.

(8) B.R. Bean, E.R. Westwater and R.L. Abbott, "Humidity and Moisture-Measurement and Control In Science and Industry", Vol. 2, Reinhold Publishing Corp., 1965, pg. 595.

(9) C.W. Allen, Ibid.

(10) A.E.S. Green and M. Griggs, App. Optics, 2, No. 6, June 1963, pg. 561.

(11) W.E.K. Middleton, "Vision Through the Atmosphere", University of Toronto Press, 1952.

(12) Ibid., pg. 110.

(13) M. Wolff, Das Licht, 8, 105-109; 128-130, 1938.

(14) K.L.S. Gunn and T.W.R. East, Quart. Jour. Roy. Meteorol. Soc., LXXX, 522-45, 1954.

(15) R.G. Medhurst, IEEE Trans. on Atennas and Propagation, AP-13, 550, 1956.

SELECTED BIBLIOGRAPHY

Preparatory to this study, a computerized literature search was conducted for the period 1962 to November 1976. We have selected those references which have a direct applicability to the goals of this study.

RADIO WAVE PROPAGATION

D.I. Maslich, Determination of Refraction in the Propagation of Electromagnetic Waves at the Earth's Surface,Geodeziia, Kartografiia I Aerofotos'emka, No. 15, 1972, pg. 46-49, in Russian.

A.P. Naumov and S.A. Zhevakin, Propagation of Centimeter, Millimeter and Submillimeter Radio Waves in the Earth's Atmosphere, (Absorption coefficients and Refractive Indices of Radio Waves in the Earth's Atmosphere),Radiofizika, 10, No. 9-10, pg.1213-1243, in Russian.

Collected Reprints, 1972-1973, Wave Propagation Laboratory (WPL) of the National Oceanic and Atmospheric Administration (NOAA) at Boulder, Colo. This third volume of collected reprints comprises work published from 1 Jan. 1972 through 31 Dec. 1973. The Papers included in this volume were selected to minimize duplication or extraneous material. Only abstracts rather than the full text of WPL of NOAA technical reports are included. Following the author index is a section listing references for further reading as well as the complete table of contents for the volume remote sensing of the troposhere, published in Aug. 1972. Avail. NTIS.

B.R. Bean and B.A. Hart, Worldwide Characteristics of Refractive Index and Climatological Effects(Climatology and Atmospheric Refraction Models for Worldwide Radio Wave Propagation),ESSA, Boulder, Colo. in Agard, Tropospheric Radio Wave Propagation, Pt. 1, Feb. 1971. Avail. NTIS.

H.W. Meredith and L.G. Rowlandson, The Effect of Meteorological Conditions on the Trade Wind Duct and Related Radio Wave Propagation(Meteorological Parameter Effect on Trade Wind Inversion and Radio Wave Propagation),Tech. Report, 1 Mar. 1969 to 28 Feb. 1970,Syracuse Univ. Research Corp., N.Y. Avail. NTIS.

L.G. Rowlandson, A Method to Determine an Effective Radio Refractivity Profile by Direct Radimetric Measurements(Interferometric Measurement of Radio Wave Refraction from Airborne Source),Feb. 1 to Sept. 1, 1968, Syracuse Univ. Research Corp., N.Y. Avail. NTIS.

Propagation and Absorption of Radio Waves in the Atmosphere and Troposphere, Transl. into English from Izv. Vyssh. Ucheb. Zaved., Radiofiz., 10, No. 9-10 1967, pg. 1213 -1243. Avail. NTIS.

SELECTED BIBLIOGRAPHY

Preparatory to this study, a computerized literature search was conducted for the period 1962 to November 1976. We have selected those references which have a direct applicability to the goals of this study.

RADIO WAVE PROPAGATION

D.I. Maslich, Determination of Refraction in the Propagation of Electromagnetic Waves at the Earth's Surface,Geodeziia, Kartografiia I Aerofotos'emka, No. 15, 1972, pg. 46-49, in Russian.

A.P. Naumov and S.A. Zhevakin, Propagation of Centimeter, Millimeter and Submillimeter Radio Waves in the Earth's Atmosphere, (Absorption coefficients and Refractive Indices of Radio Waves in the Earth's Atmosphere),Radiofizika, 10, No. 9-10, pg.1213-1243, in Russian.

Collected Reprints, 1972-1973, Wave Propagation Laboratory (WPL) of the National Oceanic and Atmospheric Administration (NOAA) at Boulder, Colo. This third volume of collected reprints comprises work published from 1 Jan. 1972 through 31 Dec. 1973. The Papers included in this volume were selected to minimize duplication or extraneous material. Only abstracts rather than the full text of WPL of NOAA technical reports are included. Following the author index is a section listing references for further reading as well as the complete table of contents for the volume remote sensing of the troposhere, published in Aug. 1972. Avail. NTIS.

B.R. Bean and B.A. Hart, Worldwide Characteristics of Refractive Index and Climatological Effects(Climatology and Atmospheric Refraction Models for Worldwide Radio Wave Propagation),ESSA, Boulder, Colo. in Agard, Tropospheric Radio Wave Propagation, Pt. 1, Feb. 1971. Avail. NTIS.

H.W. Meredith and L.G. Rowlandson, The Effect of Meteorological Conditions on the Trade Wind Duct and Related Radio Wave Propagation(Meteorological Parameter Effect on Trade Wind Inversion and Radio Wave Propagation),Tech. Report, 1 Mar. 1969 to 28 Feb. 1970,Syracuse Univ. Research Corp., N.Y. Avail. NTIS.

L.G. Rowlandson, A Method to Determine an Effective Radio Refractivity Profile by Direct Radimetric Measurements(Interferometric Measurement of Radio Wave Refraction from Airborne Source),Feb. 1 to Sept. 1, 1968, Syracuse Univ. Research Corp., N.Y. Avail. NTIS.

Propagation and Absorption of Radio Waves in the Atmosphere and Troposphere, Transl. into English from Izv. Vyssh. Ucheb. Zaved., Radiofiz., 10, No. 9-10 1967, pg. 1213 -1243. Avail. NTIS.

L.A. Berry and J.R. Johler, Propagation of Terrestrial Radio Waves of Long Wavelength,National Bureau of Standards, Central Radio Propagation Lab., Boulder, Colo.,Journal of Research, Section D, Radio Propagation,66D,Nov. to Dec. 1962, pg. 737-773.

Radio Propagation in Non-Ionixed Media,(Radio Propagation in Atmosphere, and Planetary Radio and Radar Astronomical Studies), National Academy of Sciences, National Research Council, in its Progr. in Sci. Radio, 1966, pg. 95-137.

W. Nupen, Bibiography on Tropospheric Propagation of Radio Waves,(Bibiography and Abstracts on Tropospheric Propagation of Radio Waves), National Bureau of Standards, Boulder, Colo., (Central Radio Propagation Lab.), 1 Apr., 1965, pg.346.

V.V. Novikov, Radio Wave Propagation Over a Layered Path, (Radio Wave Propagation Over a Layered Path, Accuracy of Approximate Formulas for Propagation), Joint Publications Research Service, Washington, D.C., in its Probl. of Wave Diffraction and Propagation, 1965 pg. 133-151.

W.B. Moreland, Estimating Meteorological Effects on Radar Propagation 1, (Atmospheric Refraction, Climate, and Weather Effects on Radio-Radar Wave Propagation, Bibliography), Air Weather Service, Scott AFB, Ill., Jan., 1965, pg. 207.

M.P. Dolukhanov, Procagation of Radio Waves, (Radio Wave Propagation), Air Force Systems Command, Wright, Patterson AFB.,Ohio, Foreign Technology Div.), Feb.,15,1963, pg. 502,Refs. Transl. into English from the Book"Rasprostraneniye Radiovoln", Moscow, 1 Radio , 1960, pg. 1-391.

R.M. Ring, A Theoretical Study of Tropospheric Radiowave Propagation Scientific Report No. 1,(Tropospheric Radio Wave Propagation), Boston Coll., Chestnut Hill, Mass., May 1963, pg.88.

J.H. Alt, Atmospheric Effects on Millimeter Wave Propagation, Dayton Univ. Research Inst., Ohio, Wright, Patterson, AFB, Ohio.

N. Abel and A. Sander, The Influence of the Troposphere on Ground Radio Communication at the Frequencies Above 10 GHZ., Review of the State of the Art, Air Force Systems Command, Wright, Patterson, Ohio, (Foreign Technology Div.), Transl. into English From Report of Deutsche Bundespost Fernmeldetechnisches Zentralamt Forschungsgruppe, West Germany, 1970, 44 pg..

E. Vassy, Refraction of Radioelectric Waves in the Troposphere, (Radio Wave Refraction in Troposphere), National Aeronautics and Space Administration, Washington, D.C., Transl. into English from," Physique De L'Atmosphere",Paris 1959, 2 ,pg. 95-153.

R.S. Hughes and A. Lester, Radar Wave Propagation Bibliography,(Bibliography and Abstracts on Radar Wave Propagation Emphasizing Multipath Transmission and Scattering), Naval Ordance Test Station, China Lake, Calif., June 1967, 165 pg..

MICROWAVE AND INFRARED EMISSION OF WATER-VAPOR FROM THE ATMOSPHERE

A.E. Basharinov and A.S. Gurvich, The Radio Emission of the Earth As a Planet, Moscow, Izdatel'stvo Nauka, 1974. In Russian.

M. Sovrano and B. Boldrin, Investigation on Nocturnal Radiation Measured By a New Differential Radiometer, in Heat Transfer 1974; Proceedings of the Fifth International Conference, Tokyo, Japan, Sept. 3-7, 1974,Vol. 5 (A75-14226 -03-34) Tokyo, Society of Heat Transfer of Japan, 1974, pg 303-307.

An improved differential radiometer consisting of two detector discs of identical construction but with different emissivities of their surface was used to obtain measurements of infrared radiation emitted by the sky and by earthly areas taken from two sites at different altitudes and during night-time hours. A new correlation which allowed for the evaluation of net radiation was established between atmospheric emission, water-vapor pressure and air temperature at ground level.

M.S. Malkevich, Iu. S. Georgievskii and G.V. Rozenberg, The Transparency of the Atmosphere in the Infrared, Academy of Sciences, USSR, Izvestiya, Atmospheric and Oceanic Physics, 9, Dec. 1973, pg 718-724. Translation.

A.G. Gorelik, V.V. Kalashnikov and Iu. A. Frolov, Determination of Total Atmospheric Moisture Content from Atmospheric Emission,in Advances in Satellite Meteorology, 2(A74-45060 23-30), New York, Halsted Press; Jerusalem, Israel Program for Scientific Translations, 1974, pg. 3-18. Translation.

Examination of various techniques for measuring the total water-vapor content of the atmosphere from its thermal emission in the microwave band. Problems connected with the accuracy required for radiometric measurements of total moisture content are treated. Radiosonde data are employed to compute absorption, brightness temperatures and their gradients in the 0.8 to 1.6 cm. range under different meteorological conditions for all seasons of the year. These calculations provide corresponding data on the angular and spectral distribution of atmospheric emission. Theoretical and experimental data obtained under the same meteorological conditions were compared. The measurement methods and the microwave apparatus employed for the spectral are briefly described.

A.P. Naumov, Interpretation of the Atmosphere's Radio Emission in the 5 mm Band, Academy of Sciences, USSR, Izvestiya, Atmospheric and Oceanic Physics, 9, July 1973, pg. 394-399. Translation.

The effects of H_2O, CO, O_3, N_2O, NO and clouds on the radio emission of the atmosphere in the 5 mm resonance absorption band of molecular oxygen are discussed. Considerations are given concerning the selection of suitable frequencies for determining the verical profile of brightness temperature from radar measurements of atmospheric radiation at a wavelength of about 5 mm.

T.L. Poppelbaum, Effect of Humidity on Infrared and Visual Atmospheric Transmission, General Electric Co., Aircraft Equipment Div., Utica, N.Y., in Annual Elecro-optical Systems Design Conference, New York, Sept. 12-14, 1972, Proceedings of the Technical Program (A73-18276 06-14), Chicago, Industrial and Scientific Conference Management,Inc., 1972, pg. 239-234.

Discussion of the effect that atmospheric water-vapor exerts on the transmission of visual and infrared light through the atmosphere. It is shown that moderate humidity conditions that can degrade the performance of IR equipment such as foward-looking infrared radar (FLIR) can have little or no effect on the performance of visual systems such as low light-level television (LLLTV). FLIR performance degradation can be expected to be the most pronounced when warm humid conditions prevail and a sea level optical path is involved. Under Haze conditions, IR may show some superiority but this advantage rapidly becomes insignificant in fog or rain conditions.

A.E. Basharinov, A.S. Gurevich and S.T. Igorov, Features of Microwave Passive Remote Sensing,Akademiia Nauk SSSR, Institut Radiotekhniki I Electroniki, Moscow, USSR, in international Symposium on Remote Sensing of the Environment, 7th, University of Michigan, Ann Arbor, Mich., May 17-21, 1971, Proceedings. Volume 1 (A72-11776 02-13), Ann Arbor, Univ. of Mich., 1971, pg. 119-123.

Evaluation of the possibilities for remote sensing of the earth's surface and atmosphere using microwave radiation measurements from aircraft. The advantages of such measurements compared to those of infrared and optical measurements include the possibility of making useful measurements under any meteorological conditions and the acquisition of additional geophysical information. The emittance of the surface of the ocean at microwavelengths depends on temperature, surface conditions and pollution.

B.J. Conrath, Inverse Problems in Radiative Transfer-A Review,(Inverse problems in radiative transfer applied to remote measurements of IR radiation from planetary atmospheres, noting temperature and water-vapor inversions), Oxford and Warsaw, Pergamon Press, in International Astronautical Federation, International Astronautical Congress, 18th, Belgrade, Yugoslavia, Sep. 24-30, 1967, Proceedings, Volume 2-Spacecraft Systems, Education, pg. 339-360.

W.J. Welch, A Four Channel Radiometer for Remote Sensing of Atmospheric Structure, Final Report, 1 Sep. 1970 - 1Sep. 1972, California Univ., Berkeley (Radio Astronomy Lab.).

The report describes a 4 channel radiometer system built to measure the intensity of microwave emission from atmospheric oxygen and water-vapor. The 4 channels are at 22, 51, and 59 GHz. From such measurements, the profiles of humidity and temperature in the lowest 10 kilometers of the atmosphere may be inferred. Outputs from the 4 channels are recorded continuously. The system has internal calibration sources which are automatically switched to the radiometer inputs at regular intervals. External calibration black bodies are available for periodic calibration of the internal calibration sources. Considerable effort has gone into stabilizing the internal calibration and the radiometer operating frequencies. The operation and calibration of the instrument is discussed.

B.J. Conrath, Indirect Sensing of Atmospheric Water-vapor, NASA, Goddard Spaceflight Center, Greenbelt, Md.,in its Significant Accomplishments in Science, 1968, 1969, pg. 20-22. Avail NTIS.

E.R. Westwater, Ground-Based Passive Probing Using the Microwave Spectrum of Oxygen, (Tropospheric kinetic temperature structure from ground-based measurements of oxygen emission spectra in the microwave region, using inversion technique and iterative method), NBS, Central Radio Propagation Lab., Boulder, Colo.,Journal of Research, Section D, Radio Science,69D, Sep. 1965, pg. 1201-1211.

R.L. Abbott, B.R. Bean and E.R. Westwater, Potential Use of Passive Probing of Atmospheric Structure by Thermal Emissions at Radio Frequencies,(Water-Vapor and atmospheric temperature profile determination using ground-based radiometery in the microwave region), NBS, Boulder, Colo., International Symposium on Humidity and Moisture, 1st, Washington, D.C., May 20 - 23, 1963, In- Humidity and Moisture- Measurement and Control in Science and Industry, Volume 2-Applications, Edited by E.J. Amdur., New York, Reinhold Publishing Corp., 1965, pg. 595-608.

H.J. Bolle, Investigation of the Infrared Emission Spectrum of the Atmosphere and Earth, Part II, Final Report, Ludwig-Maximilians-Universitat, Munich, West Germany, Meteorologisches Institut, 31 July, 1965. Available NTIS.

A.C. Anway and G.D. Phillips, Radiometric Vertical Sensing Technique, Final Technical Report, Mar. 1961 - July 1966, Collins Radio Co., Cedar Rapids, Iowa, Wright-Patterson AFB, Ohio AF Flight Dyn. Lab., Dec. 1966.

R.L. Abbott and E.R. Westwater, Passive Probing in the Microwave Region and Microwave Absorption Properties of Oxygen,(Atmospheric probing in the microwave region and comparison of oxygen and water-vapor microwave absorption spectrum with atmospheric thermal noise emission spectrum), NBS, Boulder, Colo., Central Radio Propagation Lab., Mar. 1965.